



Towards a sustainable hydrogen economy: Optimisation-based framework for hydrogen infrastructure development

Marta Moreno-Benito^a, Paolo Agnolucci^b, Lazaros G. Papageorgiou^{a,*}

^a Centre for Process Systems Engineering, UCL (University College London), Torrington Place, London WC1E 7JE, United Kingdom

^b UCL Institute for Sustainable Resources, UCL (University College London), 14 Upper Woburn Place, London WC1H 0NN, United Kingdom

ARTICLE INFO

Article history:

Received 15 May 2016

Received in revised form 9 August 2016

Accepted 13 August 2016

Available online 2 September 2016

Keywords:

Hydrogen economy

Infrastructure development

Multi-period spatially-explicit MILP model

Economies of scale

Hydrogen transmission and distribution

CCS

ABSTRACT

This work studies the development of a sustainable hydrogen infrastructure that supports the transition towards a low-carbon transport system in the United Kingdom (UK). The future hydrogen demand is forecasted over time using a logistic diffusion model, which reaches 50% of the market share by 2070. The problem is solved using an extension of SHIPMod, an optimisation-based framework that consists of a multi-period spatially-explicit mixed-integer linear programming (MILP) formulation. The optimisation model combines the infrastructure elements required throughout the different phases of the transition, namely economies of scale, road and pipeline transportation modes and carbon capture and storage (CCS) technologies, in order to minimise the present value of the total infrastructure cost using a discounted cash-flow analysis. The results show that the combination of all these elements in the mathematical formulation renders optimal solutions with the gradual infrastructure investments over time required for the transition towards a sustainable hydrogen economy.

© 2016 The Authors. Published by Elsevier Ltd. This is an open access article under the CC BY license (<http://creativecommons.org/licenses/by/4.0/>).

1. Introduction

The energy sector faces a moment of great challenges to move towards sustainable energy futures. Energy systems currently deal with the depletion of natural resources, volatile international oil prices, high pressures on energy security and damaged air quality in congested cities (Floudas et al., 2016). The European Union additionally set the goal of reducing 1990 greenhouse gas (GHG) emission levels below the 80% by 2050. So, decisive measures are needed to bring about low-carbon energy options. In the last decade, hydrogen has been widely discussed as a notable future alternative to replace oil and natural gas delivering high-quality and clean energy in transport and heat sectors (Marbán and Valdés-Solís, 2007). Hydrogen also has important applications in industry, energy storage from intermittent sources like solar and wind power, and stationary fuel cell systems. The relevance of hydrogen as an energy carrier is because it can be generated from a variety of primary energy sources, renewable and non-renewable, and hence it can span the several phases of a transition towards energy futures that meet sustainable goals (Ekins and Hughes, 2009). Even so, a major difficulty is the high investment required for adapting the infrastructure of energy conversion, storage, distribution and end-use

technologies, which will determine the position of hydrogen in the coming years. This way, decision-support tools for hydrogen infrastructure design and operation are necessary to evaluate its mid- and long-term economic viability and the associated mitigation of carbon emissions, so that public agencies and shareholders can back the necessary investments and policy-making processes.

In the last decade, extensive literature has emerged addressing the hydrogen supply chain (HSC) infrastructure design at different spatial scales with a diverse level of detail (Agnolucci and McDowall, 2013). In particular, the explicit representation of the hydrogen network across geographical regions is decisive to link the hydrogen production sites to the hydrogen storage and supply locations and to determine accurate hydrogen transportation requirements. Most of the works solve this problem using optimisation-based approaches with spatially-explicit mixed integer linear programming (MILP) models (Agnolucci et al., 2013; Almansoori and Shah, 2009, 2012; De-León Almaraz et al., 2014, 2015; André et al., 2014; Dayhim et al., 2014; Guillén-Gosálbez et al., 2010; Han et al., 2012, 2013; Hugo et al., 2005; Johnson and Ogden, 2012; Kamarudin et al., 2009; Kim et al., 2008; Konda et al., 2011, 2012; Li et al., 2008; Sabio et al., 2010, 2012; Samsatli et al., 2016), similarly to other contributions in bio-energy supply chains (e.g. Akgul et al., 2012; Čuček et al., 2014; d'Amore and Bezzo, 2016; Giarola et al., 2011; Marvin et al., 2013; Yue et al., 2014) and general energy systems (Liu et al., 2011). Another key element in the infrastructure

* Corresponding author.

E-mail address: l.papageorgiou@ucl.ac.uk (L.G. Papageorgiou).

Notation*Acronyms and abbreviations*

BG	biomass gasification
CCS	carbon capture and storage
CG	coal gasification
GH ₂	gas hydrogen
GHG	greenhouse gas
HSC	hydrogen supply chain
LH ₂	liquid hydrogen
MILP	mixed-integer linear programming
SHIPMod	spatial hydrogen infrastructure planning model
SMR	steam methane reforming
WE	water electrolysis

Sets

$d \in D$	diameter sizes of pipelines
$f \in F$	filling station types
$g, g' \in G$	regions
$i, i' \in I$	product types
$j \in J$	sizes of production, storage or filling facilities
$l \in L$	transportation modes
$p \in P$	production technologies
$r \in R$	reservoirs
$s \in S$	storage technologies
$t \in T$	ordered time periods
$y \in \{1, \dots, Y\}$	years in each time period

Subsets

$(g, g') \in N \subseteq G \times G$	neighbouring regions
$(g, g') \in CN \subseteq G \times G$	connections between regions for onshore CO ₂ pipelines
$(g, r) \in GR \subseteq G \times R$	connections between regions and reservoirs for offshore CO ₂ pipelines
$(i, f, j) \in IFJ \subseteq I \times F \times J$	combinations of product types, filling technologies and filling station sizes
$(l, g, g') \in LN \subseteq L \times G \times G$	connections between regions for transportation modes
$(i, p, j) \in IPJ \subseteq I \times P \times J$	combinations of product types, production technologies and plant sizes
$(i, s, j) \in ISJ \subseteq I \times S \times J$	combinations of product types, storage technologies and storage sizes
$(l, g) \in LG \subseteq L \times G$	transportation modes in regions
$(i, l) \in IL \subseteq I \times L$	combinations of product types and transportation modes
$\check{d} \in \check{D} \subseteq D$	diameter sizes of local hydrogen pipelines
$\bar{d} \in \bar{D} \subseteq D$	diameter sizes of regional hydrogen pipelines
$\underline{d} \in \underline{D} \subseteq D$	diameter sizes of onshore CO ₂ pipelines
$\underline{\underline{d}} \in \underline{\underline{D}} \subseteq D$	diameter sizes of offshore CO ₂ pipelines
$g \in P \subseteq G$	regions with major liquid freight ports

Parameters

α	annual network operating period (d y ⁻¹)
β	storage time interval (d)
γ_{ipjt}^c	coefficient of CO ₂ capture for producing product i by plant type p and size j in time period t (kg CO ₂ kg ⁻¹ H ₂)
γ_{ipjt}^e	coefficient of CO ₂ emission for producing product i by plant type p and size j in time period t (kg CO ₂ kg ⁻¹ H ₂)
δ	ratio of pipeline operating costs to capital costs
ι	maximum percentage of international hydrogen imports over the total demand (%)
Y	duration of time periods (y)

Υ^c	useful life of hydrogen and CO ₂ pipelines (y)
Υ^f	useful life of hydrogen filling stations (y)
Υ^p	useful life of hydrogen production plants (y)
Υ^s	useful life of hydrogen storage facilities (y)
Υ^t	useful life of hydrogen road transportation modes {Trailer, Tanker} (y)
$\check{a}y_{dg}^0$	initial availability of a local hydrogen pipeline of diameter size \check{d} in region g (0–1)
$\bar{a}y_{dgg'}^0$	initial availability of a regional hydrogen pipeline of diameter size \bar{d} between regions g and g' (0–1)
$\underline{a}y_{dgg'}^0$	initial availability of an onshore CO ₂ pipeline of diameter size \underline{d} between regions g and g' (0–1)
$\underline{\underline{a}}y_{dgr}^0$	initial availability of an offshore CO ₂ pipeline of diameter size $\underline{\underline{d}}$ between collection point in regions g and reservoir r (0–1)
$\check{c}c_{\check{d}}$	capital costs of a local hydrogen pipeline of diameter size \check{d} (£ km ⁻¹)
$\bar{c}c_{\bar{d}}$	capital costs of a regional hydrogen pipeline of diameter size \bar{d} (£ km ⁻¹)
$\underline{c}c_{\underline{d}}$	capital costs of an onshore CO ₂ pipeline of diameter size \underline{d} (£ km ⁻¹)
$\underline{\underline{c}}c_{\underline{\underline{d}}}$	capital costs of an offshore CO ₂ pipeline of diameter size $\underline{\underline{d}}$ (£ km ⁻¹)
crf	capital recovery factor
ct_t	carbon tax in time period t (£ kg ⁻¹ CO ₂)
dem_{gt}	total hydrogen demand in region g in time period t (kg H ₂ d ⁻¹)
dfc_t	discount factor for capital costs in time period t
dfo_t	summation of discount factors for operating costs in time period t
$\check{d}ia_{\check{d}}$	diameter of a local hydrogen pipeline of diameter size \check{d} (cm)
$\bar{d}ia_{\bar{d}}$	diameter of a regional hydrogen pipeline of diameter size \bar{d} (cm)
$\underline{d}ia_{\underline{d}}$	diameter of an onshore CO ₂ pipeline of diameter size \underline{d} (cm)
$\underline{\underline{d}}ia_{\underline{\underline{d}}}$	diameter of an offshore CO ₂ pipeline of diameter size $\underline{\underline{d}}$ (cm)
dr	discount rate (%)
dw_{il}	driver wage of road transportation mode l transporting product type i (£ h ⁻¹)
$fcap_{ij}^{\max}$	maximum capacity of a filling station of type f and size j supplying product type i (kg H ₂ d ⁻¹)
fcc_{ij}	capital cost of filling station type f and size j for product type i (£)
$\check{f}e_{il}$	local fuel economy of road transportation mode l transporting product type i within a region (km l ⁻¹)
$\bar{f}e_{il}$	regional fuel economy of road transportation mode l transporting product type i between two regions (km l ⁻¹)
fp_{il}	fuel price of road transportation mode l transporting product i (£ l ⁻¹)
ge_{il}	general expenses of road transportation mode l transporting product type i (£ d ⁻¹)
ip	price of imported liquid hydrogen (£ kg ⁻¹ H ₂)
l_{lg}	local delivery distance of hydrogen transportation mode l in region g (km)
$\bar{l}_{lgg'}$	regional delivery distance of hydrogen transportation mode l between regions g and g' (km)

$l_{gg'}$	delivery distance of an onshore CO ₂ pipeline between regions g and g' (km)
l_{-gr}	delivery distance of an offshore CO ₂ pipeline between a collection point in region g and a reservoir r (km)
l_{margin}	distance margin for establishing a direct route between two non-adjacent regions (km)
lut_{il}	load and unload time of road transportation mode l transporting product type i (h)
me_{il}	maintenance expenses of road transportation mode l transporting product type i (£ km ⁻¹)
n	economic life cycle of capital investments (y)
nf_{ifjg}^0	initial number of hydrogen filling stations of type f and size j for product type i in region g
np_{ipjg}^0	initial number of hydrogen production plants of technology p and size j producing product type i in region g
ns_{isjg}^0	initial number of hydrogen storage facilities of type s and size j storing product type i in region g
o_t	order of time period t in the ordered set \mathbb{T}
$pcap_{ipj}^{\max}$	maximum capacity of a hydrogen production plant of type p and size j producing product type i (kg H ₂ d ⁻¹)
$pcap_{ipj}^{\min}$	minimum capacity of a hydrogen production plant of type p and size j producing product type i (kg H ₂ d ⁻¹)
pcc_{ipj}	capital cost of a production plant of type p and size j producing product type i (£)
\bar{q}_d^{\max}	maximum flowrate in a local hydrogen pipeline of diameter size \bar{d} (kg H ₂ d ⁻¹)
\bar{q}_d^{\max}	maximum flowrate in a regional hydrogen pipeline of diameter size \bar{d} (kg H ₂ d ⁻¹)
\underline{q}_d^{\max}	maximum flowrate in an onshore CO ₂ pipeline of diameter size \underline{d} (kg CO ₂ d ⁻¹)
\underline{q}_d^{\max}	maximum flowrate in an offshore CO ₂ pipeline of diameter size \underline{d} (kg CO ₂ d ⁻¹)
$rcap_r^{\max}$	total capacity of reservoir r (kg CO ₂ -eq)
ri^0	initial CO ₂ inventory in reservoir r (kg CO ₂)
\overline{rvc}_{dt}	residual value of a local hydrogen pipeline of diameter size \bar{d} built in time period t , calculated at the final time (£ km ⁻¹)
\overline{rvc}_{dt}	residual value of a regional hydrogen pipeline of diameter size \bar{d} built in time period t , calculated at the final time (£ km ⁻¹)
\underline{rvc}_{dt}	residual value of an onshore CO ₂ pipeline of diameter size \underline{d} built in time period t , calculated at the final time (£ km ⁻¹)
\underline{rvc}_{dt}	residual value of an offshore CO ₂ pipeline of diameter size \underline{d} built in time period t , calculated at the final time (£ km ⁻¹)
rvf_{ifjt}	residual value of a filling station of type f and size j for product type i built in time period t , calculated at the final time (£)
rvp_{ipjt}	residual value of a hydrogen production plant of type p and size j producing product type i built in time period t , calculated at the final time (£)
rvs_{isjt}	residual value of a storage facility of type s and size j storing product type i built in time period t , calculated at the final time (£)

rvt_{ilt}	residual value of road transportation mode l of product type i acquired in time period t , calculated at the final time (£ unit ⁻¹)
$scap_{isj}^{\max}$	maximum capacity of a storage facility of type s and size j storing product type i (kg H ₂)
$scap_{isj}^{\min}$	minimum capacity of a storage facility of type s and size j storing product type i (kg H ₂)
scc_{isj}	capital cost of a storage facility of type s and size j storing product type i (£)
\widetilde{sp}_{il}	local average speed of road transportation mode l transporting product type i within a region (km h ⁻¹)
\overline{sp}_{il}	regional average speed of road transportation mode l transporting product type i between two regions (km h ⁻¹)
$tcap_{il}$	capacity of road transportation mode l transporting product type i (kg H ₂ unit ⁻¹)
tcc_{il}	capital cost of establishing a road transportation unit of transportation mode l delivering product type i (£ unit ⁻¹)
\widetilde{tma}_{il}	local availability of road transportation mode l transporting product i within a region (h d ⁻¹)
\overline{tma}_{il}	regional availability of road transportation mode l transporting product i between two regions (h d ⁻¹)
upc_{ipj}	unit production cost for producing product type i in a production plant of type p and size j (£ kg ⁻¹ H ₂)
usc_{isj}	unit storage cost for storing product type i in a storage facility of type s and size j (£ kg ⁻¹ H ₂ d ⁻¹)

Integer variables

IF_{ifjgt}	investment of new filling stations of type f and size j for product type i in region g in time period t
IP_{ipjgt}	investment of new plants of type p and size j producing product type i in region g in time period t
IS_{isjgt}	investment of new storage facilities of type s and size j storing product type i in region g in time period t
\overline{ITU}_{ilgt}	number of new transportation units of type l and product type i for local transportation by road in region g acquired in time period t
$\overline{ITU}_{ilgg't}$	number of new transportation units of type l and product type i for regional transportation by road from regions g to g' acquired in time period t
NF_{ifjgt}	number of filling stations of type f and size j for product type i in region g in time period t
NP_{ipjgt}	number of plants of type p and size j producing product type i in region g in time period t
NS_{isjgt}	number of storage facilities of type s and size j storing product type i in region g in time period t
\overline{NTU}_{ilgt}	number of transportation units of type l and product type i for local transportation by road in region g in time period t
$\overline{NTU}_{ilgg't}$	number of transportation units of type l and product type i for regional transportation by road from regions g to g' in time period t

Binary variables

\overline{AY}_{dgt}	availability of hydrogen pipelines of diameter size \bar{d} for local distribution in region g in time period t
$\overline{AY}_{dgg't}$	availability of a hydrogen pipeline of diameter size \bar{d} between regions g and g' in time period t

$\underline{AY}_{dgg't}$	availability of a onshore CO ₂ pipeline of diameter size \underline{d} between regions g and g' in time period t
\underline{AY}_{dgrt}	availability of a offshore CO ₂ pipeline of diameter size \underline{d} between collection point in region g and reservoir r in time period t
\check{Y}_{dgt}	establishment of hydrogen pipelines of diameter size \check{d} for local distribution in region g in time period t
$\bar{Y}_{dgg't}$	establishment of a hydrogen pipeline of diameter size \bar{d} between regions g and g' in time period t
$\underline{Y}_{dgg't}$	establishment of a onshore CO ₂ pipeline of diameter size \underline{d} between regions g and g' in time period t
\underline{Y}_{dgrt}	establishment of a offshore CO ₂ pipeline of diameter size \underline{d} between collection point in region g and reservoir r in time period t

Continuous variables

CEC	carbon emissions cost (£)
DEM_{igt}	total demand for product type i in region g in time period t (kg H ₂ d ⁻¹)
\check{FC}	fuel cost for local transport (£)
\bar{FC}	fuel cost for regional transport (£)
FCC	facilities capital cost (£)
FOC	facility operating cost (£)
\check{GC}	general cost for local transport (£)
\bar{GC}	general cost for regional transport (£)
IIC	international import cost (£)
IMP_{igt}	flow rate of international import of product type $i \in \{LH_2\}$ in region g in time period t (kg H ₂ d ⁻¹)
\check{LC}	labour cost for local transport (£)
\bar{LC}	labour cost for regional transport (£)
\check{MC}	maintenance cost for local transport (£)
\bar{MC}	maintenance cost for regional transport (£)
PCC	pipeline capital cost (£)
POC	pipeline operating cost (£)
PR_{ipjgt}	production rate of product type i produced by a plant of type j and size p in region g in time period t (kg H ₂ d ⁻¹)
\check{Q}_{ilgt}	local flowrate of product type i via transportation mode l in region g in time period t (kg H ₂ d ⁻¹)
$\bar{Q}_{ilgg't}$	regional flowrate of product type i via transportation mode l between regions g and g' in time period t (kg H ₂ d ⁻¹)
$\underline{Q}_{gg't}$	regional flowrate of CO ₂ via onshore pipelines between regions g and g' in time period t (kg CO ₂ d ⁻¹)
\underline{Q}_{grt}	flowrate of CO ₂ via offshore pipelines from a collection point in region g to a reservoir r in time period t (kg CO ₂ d ⁻¹)
RCC	road transportation capital cost (£)
RI_{rt}	inventory of CO ₂ in reservoir r in time period t (kg CO ₂ -eq)
ROC	road transportation operating cost (£)
ST_{isjgt}	average inventory of product type i stored in a storage facility of type s and size j in region g in time period t (kg H ₂)
TC	total supply chain cost (£)
TCC	transportation capital cost (£)
TOC	transportation operating cost (£)

planning is the distribution of hydrogen at the local scale. For the transport sector supply, this is related with the optimal siting of refuelling stations and can be solved by minimising the average distance to the filling facilities or maximising the passing traffic flows therein (Agnolucci and McDowall, 2013; Upchurch and Kuby, 2010). Although losing some degree of detail, local considerations have also been integrated in regional-scale problems based on average distances and local flowrate calculations (Agnolucci et al., 2013; Almansoori and Shah, 2012) or refining the spatial discretisation (De-León Almaraz et al., 2014). The use of MILP optimisation-based strategies for solving the infrastructure problem with regional and local scale considerations is the focus of this work.

In addition to the spatial attributes, the infrastructure optimisation also requires the definition of the network design and operation over the several phases of the transition. The adoption of hydrogen as energy carrier is a slow process that needs to overcome many social, technological and economic barriers. For instance, the transitions to new types of vehicle and fuel in the passenger transport sector are historically slow and this has important cost implications in terms of under-utilised capital, as discussed by Agnolucci and McDowall (2013). Then, the infrastructure requirements of the early years of the transition are considerably lower to the later requirements with higher hydrogen market penetration. Several of the prior studies on hydrogen infrastructure optimisation examine the spatial and temporal deployment simultaneously using multi-period spatially-explicit MILP formulations. However, only a minority perform a discounted cash flow analysis and take into account the residual value of the infrastructure, which is decisive for evaluating the economic performance with expenses incurred at different times without biasing the infrastructure deployment towards solutions with large initial investment. Likewise, given the high capital requirements, the useful life of the production, storage, filling and transportation elements has a significant influence in the infrastructure evolution, even if it is typically assumed to be infinite.

Moreover, the cost of the HSC infrastructure highly depends on the hydrogen delivery form (Yang and Ogden, 2007). The storage and transportation of hydrogen is challenging due to its low volumetric energy density at standard temperatures and pressures, thus requiring transportation technologies that increase its value. The three principal transportation methods are compressed gas trailers, cryogenic liquid tankers and gas pipelines (Dodds and McDowall, 2012). Liquid tankers are a popular alternative for delivering hydrogen at a relatively low cost with small capital expenses beforehand. Hydrogen pipelines require larger investments in advance but are the most cost-effective method of delivering large flow rates of hydrogen over short times and long distances. In contrast, compressed hydrogen road transportation is argued to be the less efficient alternative, but necessary for carrying small hydrogen amounts over short distances during the first years of the transition. Many of the above mentioned works include compressed or liquid road transportation, quantifying the number of transportation units based on the mathematical formulation by Almansoori and Shah (2009). Hydrogen delivery via pipelines has been also studied (Johnson and Ogden, 2012; Samsatli et al., 2016). However, the efforts for simultaneously considering pipelines and road transportation modes (André et al., 2014; Han et al., 2012, 2013; Kim et al., 2008; Konda et al., 2011; Sabio et al., 2010, 2012) are critical for the study of the infrastructure evolution in transition timeframes.

Hydrogen can be obtained from several primary energy sources, including intermittent renewable sources and biomass, as well as coal and natural gas. Since there is still a high presence of fossil resources as a cost-effective feedstock, while renewable source infrastructures like wind and solar farms continue developing,

it is necessary to isolate the CO₂ emissions by means of carbon sequestration technologies. Significant research has been devoted to the study of hydrogen production with CO₂ capture (Voldsund et al., 2016) and the modelling of carbon capture and storage (CCS) networks that connect carbon sources and geologic storage reservoirs via pipelines (Elahi et al., 2014; Middleton and Bielicki, 2009). However, few works address the HSC optimisation while accounting for the costs of CCS technologies in hydrogen production from fossil fuels (Han et al., 2013; Konda et al., 2011) and less contributions integrate the simultaneous optimisation of CCS pipelines and reservoirs (Agnolucci et al., 2013). Specifically, the trade-off between the hydrogen and CCS networks is an important factor in the optimal spatial structure of the hydrogen system.

Finally, economies of scale represent cost advantages that are obtained depending on the production size; this means decreasing capital costs per hydrogen production/transportation rate for increasing capacities. In particular, the comparison of multiple hydrogen production data illustrates a decrease in the capital cost per production rate with the increase of the plant size. Scales in production have been considered by some contributions in the state-of-the-art (Agnolucci et al., 2013; Almansoori and Shah, 2009, 2012; De-León Almaraz et al., 2014, 2015; Johnson and Ogden, 2012; Konda et al., 2011, 2012) and are necessary for comparing the advantages of centralised versus distributed production, as well as the impact in the transportation costs.

Even though most of the aspects of the HSC infrastructure have been covered in the literature, there is no reported formulation for optimising simultaneously the range of production technologies, scales, transportation modes and CCS elements across time and space. Such an approach will be required to manage a gradual penetration of hydrogen demand and tightening CO₂ emission budgets. So, an open question that remains under discussion is how the hydrogen infrastructure will back the transition towards long-term sustainable hydrogen economies while guaranteeing short- and mid-term system manoeuvrability, starting from current carbon-based economy. In this work, we present an optimisation-based framework consisting of a multi-period spatially-explicit MILP formulation that solves the hydrogen infrastructure development over changing timeframes. The mathematical formulation extends a previous model proposed by the authors (Agnolucci et al., 2013) and includes road transportation of liquid and compressed hydrogen, and small/distributed production scales – for earlier phases of the transition – and high-capacity hydrogen pipelines and medium/large production plants – for later phases. Hydrogen production from fossil fuels and biomass, with and without carbon capture, and from renewable electricity is considered, together with international imports. Hydrogen delivery is quantified at local and regional levels. The optimisation of the CO₂ pipelines and reservoir levels is also included in the formulation. Moreover, a discounted cash flow analysis with residual values and equipment useful life is performed. By optimising all these decisions simultaneously, it is possible to evaluate the trade-off among all the infrastructure alternatives over time.

The remaining of this paper is organised as follows: The problem statement and hydrogen pathways are presented in Section 2 and the mathematical model is described in Section 3. Section 4 details the hierarchical procedure used for solving the optimisation problem. A case study tackling the hydrogen infrastructure optimisation for the passenger sector in the UK is presented in Section 5 and the results are discussed in Sections 6–8. There, the role of the diverse elements included in the optimisation framework is evaluated by comparing several scenarios with different economic, delivery, CCS and hydrogen import assumptions. Finally, the concluding remarks are drawn in Section 9.

2. Problem statement

The goal of this work is to design optimal HSC infrastructures over a planning horizon in order to satisfy the growing hydrogen demand and tightening GHG emission targets that characterise the transition towards a sustainable hydrogen economy. The optimisation problem includes design decisions regarding the location, technology and scale of hydrogen production plants, storage facilities and filling stations, as well as the selection, capacity and connectivity of hydrogen transportation modes, the characterisation of the CCS system and the definition of international imports. The problem is formalised as follows. Given:

- the hydrogen demand per region and time period over a fixed time horizon;
- the set of available hydrogen production, storage and filling technologies for liquid and compressed product forms, as well as their capacity at different scales;
- the set of connections between regions, the set of local and regional hydrogen transportation modes, the delivery distance in each region and between regions, and the capacity of road transportation units and hydrogen pipelines with different diameters;
- the CO₂ emission and capture factors, the set of regions with CO₂ collection points, the distance between regions and from collection points to reservoirs for onshore and offshore CO₂ pipelines, and the capacity of reservoirs and CO₂ pipelines with different diameters;
- the set of regions with major liquid freight ports;
- the capital and unit processing costs of each technology type, transportation mode and scale, the carbon tax, the price of liquid hydrogen imports, the interest rate and the residual values at the end of the time horizon;

the goal is to determine:

- the endogenous relation of liquid and compressed hydrogen demand;
- the location, type, scale and number of hydrogen production plants, storage facilities and filling stations, as well as the hydrogen production rates and stored amounts;
- the connections between regions, hydrogen transportation modes, transportation units, pipeline diameters and flowrates of local and regional hydrogen supply;
- the connections, pipeline diameters, and flowrates of onshore and offshore CO₂ pipelines, as well as inventory levels of CO₂ reservoirs;
- the international import of liquid hydrogen in each freight port;

such that the total cost of the HSC infrastructure is minimised, including the discounted capital and operating costs of facilities, road transportation units, hydrogen and CO₂ pipelines, carbon emission costs, and expenditure on international imports, as well as their corresponding residual values.

The adaptability of the supply chain is leveraged in this study by considering several production technologies, transportation modes, economies of scale and product forms. Fig. 1 summarises the hydrogen and CO₂ pathways included in the optimisation framework. It shows the versatility of hydrogen as an energy carrier, as it can be obtained from several production technologies and primary energy sources, including water electrolysis (WE), powered by a grid mix inclusive of intermittent renewable sources, steam methane reforming (SMR), and the gasification of coal (CG) or biomass (BG). While renewable energy technology continues developing, fossil resources can be used as a cheaper feedstock. However, to adapt the hydrogen production to the available primary energy sources without jeopardising the reduction of carbon

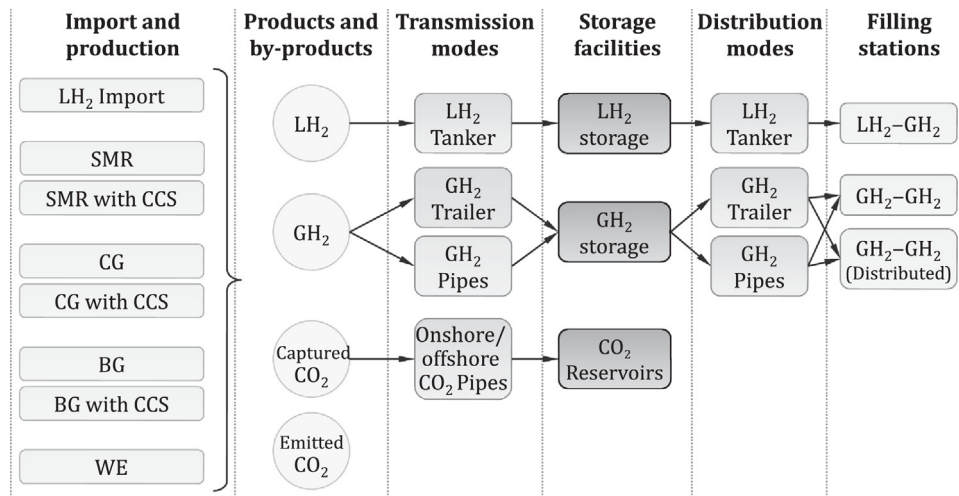


Fig. 1. Hydrogen and CO₂ pathways included in the optimisation framework.

emissions, a part of CO₂ emissions should be isolated through CCS technologies and transported to sub-sea reservoirs via onshore and offshore pipelines. Specifically, SMR with post-combustion capture and CG/BG with pre-combustion capture, including water gas shift reaction and a physical separation process like adsorption, are considered. This framework focuses on CO₂ sequestration, and other gases like CO, CH₄, or N₂O are out of the scope. Another pathway examined here is the international import of liquid hydrogen. This alternative helps to fulfil increasing hydrogen demands while reducing the under-utilised capital in the early phases of the transition through the delay of some large-scale investments.

The suitability of hydrogen delivery options depends on the hydrogen market penetration and, therefore, is likely to change over time. The three transportation methods considered here are GH₂ trailers, LH₂ tankers and GH₂ pipelines. Road transportation of liquid hydrogen is a relevant alternative for short distances and small volumes, whereas gas pipelines are the most cost-effective transmission mode for long distances and large hydrogen flowrates. However, they present significant economies of scale, so road transportation of compressed hydrogen can be used as a more flexible backup in early periods. Hence, it is essential to include the production, transportation and storage of both liquid and gas hydrogen forms. In all cases, it is produced and warehoused in a strategic distribution site in each region, which is connected to other areas through transmission routes. From there, hydrogen is distributed locally to scattered demand centres for its supply. Three types of filling stations are considered, *i.e.* LH₂–GH₂ stations receiving hydrogen by tanker, GH₂–GH₂ stations receiving hydrogen by trailer or pipe, and GH₂–GH₂ stations with on-site production.

3. Mathematical model

The hydrogen infrastructure development problem is solved using an extension of the mathematical programming framework ‘spatial hydrogen infrastructure planning model’ (SHIPMod) proposed by Agnolucci et al. (2013), which consists of a multi-period spatial-explicit MILP model. Such an optimisation-based framework is enhanced in this work in several ways. First, the extension incorporates the useful life of the infrastructure elements to represent accurately transition horizons (Section 3.2). Second, the extended framework considers additional hydrogen delivery modes – *i.e.* transmission and distribution pipelines – (Section 3.6) and international imports (Section 3.7), which are key elements in the mid- and long-term transition towards a hydrogen future.

Third, road transportation units are now defined by integer variables instead of continuous ones (Section 3.5). Fourth, the local transportation assumptions are modified to consider hydrogen distribution from a central distribution site – where the hydrogen is either produced or introduced from other regions – to dispersed filling stations in each region (Section 3.3). Finally, another improvement is the revision of the regional transportation constraints to adopt a ‘neighbourhood flow’ approach (Akgul et al., 2011) that allows long-distance hydrogen transmission through intermediate regions (Section 3.4).

3.1. Model overview

The detailed HSC superstructure in each geographical region $g \in G$ and reservoir $r \in R$ in period $t \in T$ is illustrated in Fig. 2. The different components are detailed next. The values of all the model parameters are gathered in the Supplementary Material.

Hydrogen production and import. The superstructure starts with a set of hydrogen production technologies, with and without carbon capture:

$P = \{\text{SMR, SMR-CCS, CG, CG-CCS, BG, BG-CCS, WE}\}$. Each of these technologies can be designed at different production scales:

$J = \{\text{Distributed, Small, Medium, Large}\}$, and generates hydrogen in liquid (LH₂) or gas (GH₂) physical forms and CO₂, which is emitted to the atmosphere or isolated with CCS technologies. The CO₂ outflows are calculated with emission and capture factors γ_{ipjt}^e and γ_{ipjt}^c , which assume that all the CO₂ generated in the conversion process can be separated, unlike the one associated with electricity consumption. The total emissions are penalised with a carbon tax (ct_t). The combination of production technologies and scales for each product form is defined by the subset $IPJ \subseteq I \times P \times J$. The hydrogen production rate (PR_{ipjgt}) in each period and region is constrained by the number of available plants (NP_{ipjgt}), characterised by minimum and maximum capacities ($pcap_{ipj}^{\min}$ and $pcap_{ipj}^{\max}$), capital cost (pcc_{ipj}) and unit production expenses (upc_{ipj}), inclusive of liquefaction and carbon capture technologies. Alternatively, LH₂ can be imported from overseas with a price (ip) and flowrate (IMP_{igt}) in the set of regions $P \subseteq G$ with major liquid freight ports.

Hydrogen transmission. Hydrogen can be transferred between neighbouring regions ($g, g' \in N$) at a regional scale. The transportation modes considered in this framework are:

$L = \{\text{Tanker, Trailer, Pipe}\}$. The combination of hydrogen physical forms and delivery modes is represented by the subset

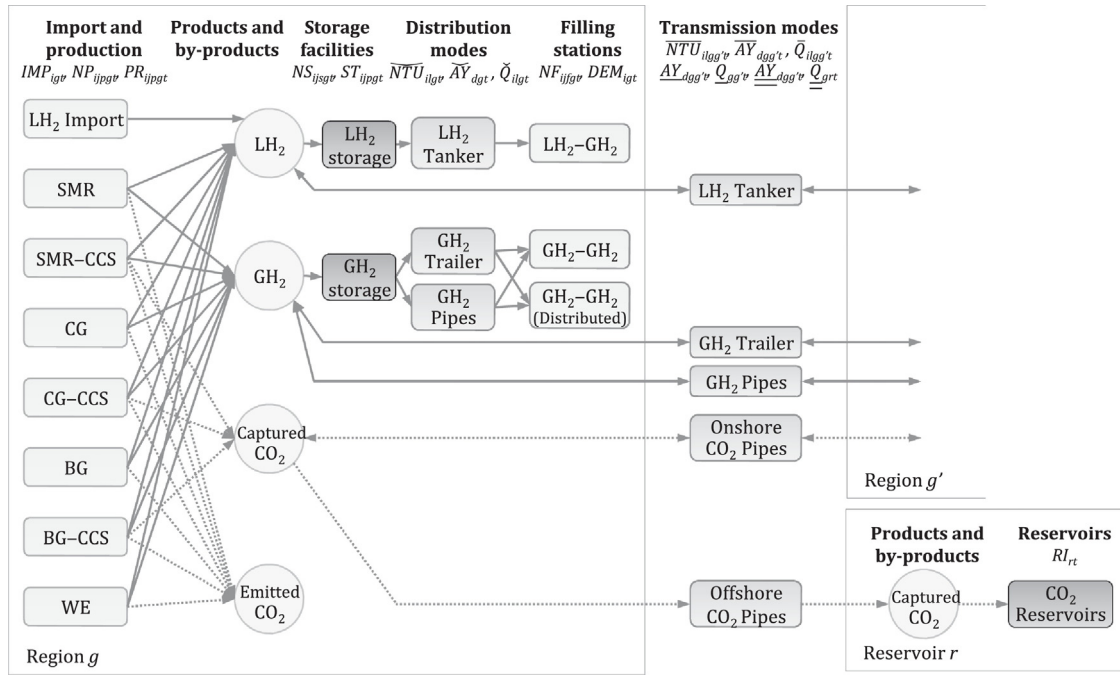


Fig. 2. Superstructure of the HSC infrastructure for each region g and reservoir r in period t addressed in the optimisation framework.

$IL \subseteq I \times L$. Additionally, the subset $LN \subseteq L \times G \times G$ denotes the possible delivery forms for each connection. Hydrogen transmission is defined by regional flowrates ($\bar{Q}_{ilgg't}$). In road transport, this variable is determined by the number of transportation units ($\bar{NTU}_{ilgg't}$) and their capacity ($tcap_{il}$), as detailed in Section 3.5. Moreover, road delivery costs are related with parameters like the regional delivery distance ($l_{ilgg'}$), driver wage (dw_{il}), fuel price (fp_{il}), general (ge_{il}) and maintenance (me_{il}) expenses, load and unload time (lut_{il}), fuel economy (fe_{il}), average speed (\bar{sp}_{il}), availability (\bar{tm}_{il}), and capital cost of establishing a new road transportation unit (tcc_{il}). In pipeline transportation, hydrogen flowrate is constrained by the availability ($\bar{AY}_{dgg't}$) of a pipe of diameter \bar{dia}_d , $d \in \bar{D}$ and its maximum flowrate (\bar{q}_d^{\max}), where typical pressure drops and pipe lengths are considered implicitly. The associated economic parameters consist of the capital cost per kilometre (\bar{ccc}_d) and the ratio of operating costs to capital expenses (δ), as explained in Section 3.6.

Storage facilities. Each region has a central warehouse for hydrogen storage using established technologies, namely cryogenic liquid and compressed gas storage:

$s = \{\text{LH}_2 \text{ Storage, GH}_2 \text{ Storage}\}$. The combination of potential technologies and scales for each product form is defined by the subset $ISJ \subseteq I \times S \times J$. The average inventory levels (ST_{isjgt}) in each region and time interval are constrained by the number of available facilities (NS_{isjgt}) and are designed to cover the hydrogen demand (DEM_{igt}) corresponding to a predefined storage period (β), which is used to accommodate plant interruptions and fluctuations in supply and demand. Each type of storage facility is characterised by a minimum and maximum capacity ($scap_{isj}^{\min}$ and $scap_{isj}^{\max}$), capital cost (scc_{isj}) and unit storage expenses (usc_{isj}).

Hydrogen distribution. The transportation modes for local hydrogen distribution are the same than regional transmission modes and are represented in each region by the subset $LG \subseteq L \times G$. Likewise, local transportation is defined by local hydrogen flowrates (\bar{Q}_{ilgt}), the number of road transportation units (\bar{NTU}_{ilgt}) and availability of local hydrogen pipelines (\bar{AY}_{dgt}) of diameter \bar{dia}_d , $d \in \bar{D}$.

Filling stations. Hydrogen for the transport sector is supplied in filling facilities of the following types:

$F = \{\text{LH}_2\text{-GH}_2, \text{GH}_2\text{-GH}_2, \text{GH}_2\text{-GH}_2 \text{ (distributed)}\}$. The combination of technologies and scales for each product form is defined by the subset $IFJ \subseteq I \times F \times J$. Given the total hydrogen demand dem_{gt} , the fraction of liquid and gas (DEM_{igt}) is an endogenous decision linked to several factors like production scales and hydrogen transportation requirements and is limited by the number of available facilities (NF_{ifjgt}) with a maximum capacity ($fcap_{ifj}^{\max}$) and capital cost (fcc_{ifj}).

CO₂ transmission. The optimisation framework also includes the planning of onshore CO₂ pipelines between neighbouring connections ($g, g' \in \text{CN} \subseteq G \times G$) and offshore pipelines between regions with CO₂ collection points and reservoirs ($g, r \in \text{GR} \subseteq G \times R$). Like in the case of hydrogen transmission, onshore and offshore CO₂ transportation is characterised by flowrates ($\bar{Q}_{gg't}$ and \bar{Q}_{grt}) and availability of pipelines ($\bar{AY}_{dgg't}$ and \bar{AY}_{dgrt}) of diameters \bar{dia}_d , $d \in \bar{D}$ and \underline{dia}_d , $d \in \underline{D}$, respectively.

CO₂ reservoirs. The CO₂ is sequestered in sub-sea reservoirs $r \in R$. Their inventory level (RI_{rt}) is constrained by the maximum capacity ($rcap_{rt}^{\max}$).

Objective function. The optimisation framework seeks to minimise the discounted total cost (TC), including capital investments to install new facilities (FCC) and the corresponding operating costs (FOC , capital expenditure (TCC) and operating costs (TOC) of hydrogen and CO₂ transportation, carbon emissions costs (CEC), and international import expenses (IIC), as follows:

$$TC = FCC + TCC + FOC + TOC + CEC + IIC, \quad (1)$$

where transportation costs are composed of road delivery and pipeline contributions ($TCC = RCC + PCC$ and $TOC = ROC + POC$). In addition to performing a discounted cash flow analysis in each period t , the residual values of infrastructure capital assets at the end of the planning horizon t^e are deducted. These are calculated using the sum-of-years-digits depreciation function.

The complete multi-period spatial-explicit MILP formulation of SHIPMod expansion is presented in the Supplementary Material. The extensions of the formulation by Agnolucci et al. (2013) newly addressed in this work are detailed next.

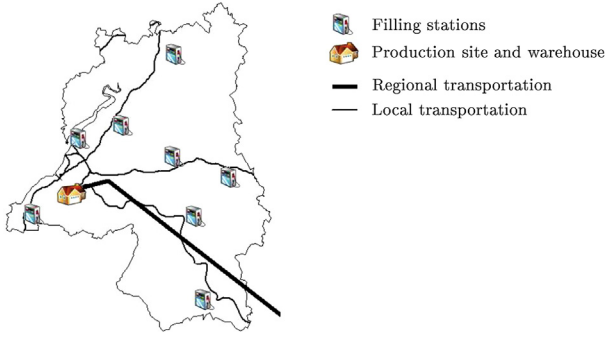


Fig. 3. Local transportation with central warehouses and distributed filling stations.

3.2. Useful life and equipment availability

The availability of production, storage, filling station facilities and transportation modes is subject to the useful life of the equipment. For instance, the number of production plants (NP_{ipjgt}) in region g during period t is determined by the available plants in the preceding period $t-1$, the number of newly installed facilities in t and the ones installed in $t-t^p$, whose useful life Υ^p has finished:

$$NP_{ipjgt} = NP_{ipjg,t-1} + IP_{ipjgt} - IP_{ipjg,t-t^p_{ipj}}, \forall (i, p, j) \in IPJ, \quad g \in G, t \in T, \quad (2)$$

where t^p_{ipj} is equal to Υ^p/Υ , where Υ is the number of years in each period. The number of plants in $t-1$ in the first interval corresponds to the zero condition, i.e. the plants that have been installed before the planning horizon under study. Equivalent equations are defined to determine the number of storage facilities (NS_{isjgt}), filling stations (NF_{ifjgt}), and local and regional hydrogen road transportation units (\overline{NTU}_{ilgt} and $\overline{NTU}_{ilgg't}$) in region g or between regions g and g' , with lifetimes Υ^s , Υ^f and Υ^t , respectively. Likewise, the availability of hydrogen (\overline{AY}_{dgt} and $\overline{AY}_{dgg't}$) and CO₂ pipelines ($\overline{AY}_{dgg't}$ and \overline{AY}_{dgrt}) in region g , or between regions g and g' or reservoir r , is defined by analogous equations with a lifetime Υ^c . These constraints are detailed in the Supplementary Material (Eqs. S30, S33, S36, S39, S40, and S45–S48).

3.3. Local transportation assumptions

Local hydrogen distribution in each region is assumed to be transported from a central warehouse, located in a highly populated city, to dispersed filling stations, as shown in Fig. 3. Therefore, the total hydrogen flowrate at the local level (\check{Q}_{ilgt}) equals the hydrogen demand supplied in filling stations (DEM_{igt}) and can be carried via road transportation or via pipelines according to:

$$DEM_{igt} = \sum_{\substack{l:(i,l) \in IL \\ \wedge (l,g) \in LG}} \check{Q}_{ilgt}, \quad \forall i \in I, g \in G, t \in T. \quad (3)$$

Regarding the local delivery distances (\check{l}_{ig}), these are calculated as the geometrical radius of the total area of each region g . For practical purposes, this local arrangement affects the calculation of the delivery costs, the number of road transportation units and the pipeline

capacity requirements. For instance, the local fuel cost is calculated as follows:

$$\check{FC} = \sum_{t \in T} \sum_{l \in \{\text{Trailer}, g:(l,g) \in LG\}} \sum_{i:(i,l) \in IL} \text{Tanker} \, dfo_t \alpha f_{p_{il}} \frac{2\check{l}_{ig} \check{Q}_{ilgt}}{f_{e_{il}} tcap_{il}}, \quad (4)$$

where dfo_t is the summation of discount factors for operating costs, whose calculation is detailed in the Supplementary Material (Eq. S4), and α is the annual operating period. Other operating road expenses are the general (\check{GC}), labour (\check{LC}) and maintenance (\check{MC}) costs, which are calculated similarly, as detailed in the Supplementary Material (Eqs. S13, S15, S17 and S19). The number of delivery units and their purchase cost also depend on local flowrates and distances, as presented in Section 3.5. As for local hydrogen pipes, their expenses are determined by the pipeline length and diameter, with the latter being selected according to the maximum flowrate capacity as explained in Section 3.6.

3.4. Regional transportation assumptions

The ‘neighbourhood flow’ approach (Akgul et al., 2011) consists of the definition of a subset of connections $(g, g') \in \mathbb{N} \subset G \times G$ where each region $g \in G$ is only linked to divisions $g' \in G$ characterised by being adjacent, as opposed to a full connectivity matrix $G \times G$ where all regions are connected, which would increase the combinatorial part of the problem. With this strategy, a material can flow from the origin to the destination point by the addition of sequential neighbourhood flows (Agnolucci et al., 2013). Even though a long-distance flow through intermediate regions is devised as an essential feature, many previous contributions addressing the HSC problem have constrained this capability by forcing all the input hydrogen flowrates to a region to be consumed in that region. The optimisation framework presented here allows the product to flow through intermediate regions as it does not define any constraints on input flowrates.

3.5. Road transportation units

Hydrogen road transportation takes place through a discrete number of GH₂ trailers and LH₂ tankers at both local and regional scales. The number of transportation units (\overline{NTU}_{ilgt} and $\overline{NTU}_{ilgg't}$) required for moving hydrogen type i via road transportation mode l in region g or between regions g and g' in period t has to be able to carry hydrogen flowrates (\check{Q}_{ilgt} and $\check{Q}_{ilgg't}$) and is subject to the go and return distances ($2\check{l}_{ig}$ and $2\check{l}_{ilgg'}$), the unit capacity ($tcap_{il}$), the transportation mode availability (\overline{tma}_{il} and \overline{tma}_{il}), the average speed (\overline{sp}_{il} and \overline{sp}_{il}) and the load and unload time (lut_{il}) as follows:

$$\overline{NTU}_{ilgt} \geq \frac{\check{Q}_{ilgt}}{\overline{tma}_{il} tcap_{il}} \left(\frac{2\check{l}_{ig}}{\overline{sp}_{il}} + lut_{il} \right), \quad \forall l \in \{\text{Trailer}, \text{Tanker}\}, \quad i:(i,l) \in IL, g:(l,g) \in LG, t \in T, \quad (5)$$

$$\overline{NTU}_{ilgg't} \geq \frac{\check{Q}_{ilgg't}}{\overline{tma}_{il} tcap_{il}} \left(\frac{2\check{l}_{ilgg'}}$$

The number of available delivery units depends on the purchased units (\overline{ITU}_{ilgt} and $\overline{ITU}_{ilgg't}$) in each period, with a useful life Υ^t , according to evolution constraints similar to Eq. (2) (Eqs. S39–S40 of the Supplementary Material). The road capital cost (RCC) associated with the acquisition of new trailers and tankers is part of the

total infrastructure expenses assumed by the investor, and is calculated from the capital cost (tcc_{it}) of each unit in period t minus the residual value (rvt_{ilt}) at the end of the planning horizon t^e :

$$\begin{aligned} RCC = & \sum_{t \in T} \sum_{l \in \{\text{Trailer}, \text{Tanker}\}} \sum_{g:(l,g) \in LG} \sum_{i:(i,l) \in IL} (dfc_t tcc_{il} - dfc_{t^e} rvt_{ilt}) \overline{ITU}_{ilgt} \\ & + \sum_{t \in T} \sum_{l \in \{\text{Trailer}, \text{Tanker}\}} \sum_{(g,g'):(l,g,g') \in LN} \sum_{i:(i,l) \in IL} (dfc_t tcc_{il} - dfc_{t^e} rvt_{ilt}) \\ & \times \overline{ITU}_{ilgg't}, \end{aligned} \quad (7)$$

where dfc_t and dfc_{t^e} are the discount factors for capital costs in period t and final time t^e , whose calculation is detailed in the Supplementary Material (Eq. S3).

3.6. Hydrogen and CO₂ pipelines

Compressed hydrogen can also be transferred at local and regional levels via distribution and transmission pipelines. Moreover, onshore and offshore CO₂ pipelines are required for carrying the CO₂ captured in hydrogen production plants to sub-sea reservoirs. The availability of pipelines of diameter size $d \in \underline{D}, \overline{D}, \underline{D}$ or \underline{D} in region g , or between regions g and g' or reservoir r in period t is represented by binary variables \overline{AY}_{dgt} , $\overline{AY}_{dgg't}$, $\underline{AY}_{dgg't}$ and \underline{AY}_{dgrt} for each type of pipeline. Then, hydrogen and CO₂ flowrates (\underline{Q}_{ilgt} , $\overline{Q}_{ilgg't}$, $\underline{Q}_{gg't}$, \underline{Q}_{grt}) are limited by the maximum capacity of the selected diameter (\underline{q}_d^{\max} , \overline{q}_d^{\max} , \underline{q}_d^{\max} , \underline{q}_d^{\max}):

$$\begin{aligned} \underline{Q}_{ilgt} \leq & \sum_{d \in \underline{D}} \underline{q}_d^{\max} \overline{AY}_{dgt}, \quad \forall l \in \{\text{Pipe}\}, i \in \{\text{GH}_2\}, \\ & g : (l, g) \in LG, t \in T, \end{aligned} \quad (8)$$

$$\begin{aligned} \overline{Q}_{ilgg't} \leq & \sum_{d \in \overline{D}} \overline{q}_d^{\max} \overline{AY}_{dgg't}, \quad \forall l \in \{\text{Pipe}\}, i \in \{\text{GH}_2\}, \\ & (g, g') : (l, g, g') \in LN, t \in T, \end{aligned} \quad (9)$$

$$\underline{Q}_{gg't} \leq \sum_{d \in \underline{D}} \underline{q}_d^{\max} \underline{AY}_{dgg't}, \quad \forall (g, g') \in CN, t \in T, \quad (10)$$

$$\underline{Q}_{grt} \leq \sum_{d \in \underline{D}} \underline{q}_d^{\max} \underline{AY}_{dgrt}, \quad \forall (g, r) \in GR, t \in T. \quad (11)$$

Only one diameter size d can be installed for any type of pipelines over the whole timeframe:

$$\sum_{d \in \underline{D}} \overline{AY}_{dgt} \leq 1, \quad \forall g : (\text{Pipe}, g) \in LG, t \in T, \quad (12)$$

$$\sum_{d \in \overline{D}} \overline{AY}_{dgg't} \leq 1, \quad \forall (g, g') : (\text{Pipe}, g, g') \in LN, t \in T, \quad (13)$$

$$\sum_{d \in \underline{D}} \underline{AY}_{dgg't} \leq 1, \quad \forall (g, g') \in CN, t \in T, \quad (14)$$

$$\sum_{d \in \underline{D}} \underline{AY}_{dgrt} \leq 1, \quad \forall (g, r) \in GR, t \in T. \quad (15)$$

Pipeline availability depends on the installed pipes in each period (\overline{Y}_{dgt} , $\overline{Y}_{dgg't}$, $\underline{Y}_{dgg't}$ and \underline{Y}_{dgrt}) with a useful life Υ^c , according to evolution constraints equivalent to Eq. (2) (Eqs. S45–S48 of the Supplementary Material). The newly installed pipeline sections determine their total capital cost (PCC) as a function of the pipe diameter and length. In particular, PCC is calculated taking into account the capital cost per kilometre of pipelines with diameter size d (\overline{ccc}_d , \overline{ccc}_d , \underline{ccc}_d and \underline{ccc}_d) in period t minus the residual values per length unit (\overline{rvc}_{dt} , \overline{rvc}_{dt} , \underline{rvc}_{dt} and \underline{rvc}_{dt}) at the end of the planning horizon t^e .

$$\begin{aligned} PCC = & \sum_{t \in T} \sum_{l \in \{\text{Pipe}\}} \sum_{g:(l,g) \in LG} \sum_{d \in \underline{D}} (dfc_t \overline{ccc}_d - dfc_{t^e} \overline{rvc}_{dt}) \overline{l}_{lg} \overline{Y}_{dgt} \\ & + \sum_{t \in T} \sum_{l \in \{\text{Pipe}\}} \sum_{(g,g'):(l,g,g') \in LN} \sum_{d \in \overline{D}} (dfc_t \overline{ccc}_d - dfc_{t^e} \overline{rvc}_{dt}) \overline{l}_{lgg'} \overline{Y}_{dgg't} \\ & + \sum_{t \in T} \sum_{(g,g') \in CN} \sum_{d \in \underline{D}} (dfc_t \underline{ccc}_d - dfc_{t^e} \underline{rvc}_{dt}) \underline{l}_{gg'} \underline{Y}_{dgg't} \\ & + \sum_{t \in T} \sum_{(g,r) \in GR} \sum_{d \in \underline{D}} (dfc_t \underline{ccc}_d - dfc_{t^e} \underline{rvc}_{dt}) \underline{l}_{gr} \underline{Y}_{dgrt}, \end{aligned} \quad (16)$$

where \overline{l}_{lg} , $\overline{l}_{lgg'}$, $\underline{l}_{gg'}$ and \underline{l}_{gr} denote the distance of hydrogen and CO₂ pipeline connections. The pipeline operating cost (POC) comprises labour, administration and maintenance expenses. Energy consumption is not included because compression requirements to guarantee pipeline input and output pressures are assumed to be part of the hydrogen production facilities and filling stations. Thus, the operating cost is calculated as a proportion (δ) of capital expense annuities as follows:

$$\begin{aligned} POC = & \sum_{t \in T} \sum_{l \in \{\text{Pipe}\}} \sum_{g:(l,g) \in LG} \sum_{d \in \underline{D}} dfo_t \delta crf \overline{ccc}_d \overline{l}_{lg} \overline{AY}_{dgt} \\ & + \sum_{t \in T} \sum_{l \in \{\text{Pipe}\}} \sum_{(g,g'):(l,g,g') \in LN} \sum_{d \in \overline{D}} dfo_t \delta crf \overline{ccc}_d \overline{l}_{lgg'} \overline{AY}_{dgg't} \\ & + \sum_{t \in T} \sum_{(g,g') \in CN} \sum_{d \in \underline{D}} dfo_t \delta crf \underline{ccc}_d \underline{l}_{gg'} \underline{AY}_{dgg't} \\ & + \sum_{t \in T} \sum_{(g,r) \in GR} \sum_{d \in \underline{D}} dfo_t \delta crf \underline{ccc}_d \underline{l}_{gr} \underline{AY}_{dgrt}, \end{aligned} \quad (17)$$

where crf is the capital recovery factor, whose calculation is detailed in the Supplementary Material (Eq. S5).

3.7. International import

The total international import of LH₂ is constrained by the following equation:

$$\sum_{g \in P} \sum_{i \in \{\text{LH}_2\}} IMP_{igt} \leq \iota \sum_{g \in G} dem_{gt}, \quad \forall t \in T, \quad (18)$$

where ι is the percentage of hydrogen that can be purchased abroad over the total demand in each period t . The cost of imported hydrogen (IIC) is calculated as a function of the price (ip) and inflow (IMP_{igt}) of overseas LH₂ in time interval t and port region $g \in P$:

$$IIC = \sum_{t \in T} \sum_{g \in P} \sum_{i \in \{\text{LH}_2\}} dfo_t \alpha ip IMP_{igt}. \quad (19)$$

3.8. Model summary

Summarising, the overall optimisation problem is formulated as a multi-period spatial-explicit MILP composed of the following equations, which are detailed above and in the Supplementary Material:

$$\begin{aligned}
 &\text{Minimise } \text{Objective function TC (Eqs. 1, 7, 16–17, 19, S6–S8, S11–S20, S22)} \\
 &\text{s.t. } \text{Demand constraints (Eqs. 3, S24)} \\
 &\quad \text{H}_2 \text{ and CO}_2 \text{ Mass balance constraints (Eqs. S26–S27)} \\
 &\quad \text{Production constraints (Eqs. 2, S28–S29)} \\
 &\quad \text{Storage constraints (Eqs. S31–S33)} \\
 &\quad \text{Filling station constraints (Eqs. S34–S36)} \\
 &\quad \text{Road transportation constraints (Eqs. 5–6, S39–S40)} \\
 &\quad \text{Pipeline constraints (Eqs. 8–15, S45–S48)} \\
 &\quad \text{Reservoir constraints (Eqs. S53–S54)} \\
 &\quad \text{Hydrogen import constraints (Eq. 18)} \\
 &\quad x \in \mathbb{R}, X \in \mathbb{N}, Z \in \{0, 1\}.
 \end{aligned} \tag{20}$$

Here, x represents the continuous variables of the problem, fully detailed in the notation (*i.e.* production and import rates, storage and inventory levels, demand per product type, and hydrogen and CO₂ flowrates), X stands for integer variables (*i.e.* the number of production, storage and filling facilities and the number of transportation units) and Z denotes the binary variables (*i.e.* availability of hydrogen and CO₂ pipelines).

4. Solution procedure

Due to the large number of combinations of technologies, scales and product forms in the HSC infrastructure decisions, the resulting MILP problem is liable to become computationally intensive. Specifically, hydrogen production plants ($|IPJ|=28$), storage facilities ($|ISJ|=6$), filling stations ($|IFJ|=7$), road transportation modes ($|IL|=2$), and pipelines ($|D|=2$, $|\bar{D}|=3$, $|\underline{D}|=2$, $|\bar{D}|=2$) must be evaluated in each region ($|G|=36$, $|LG|(\text{Trailer, Tanker, Pipe})=36$) or between regions ($|LN|(\text{Trailer, Tanker})=244$, $|LN|(\text{Pipe})=152$, $|CN|=152$, $|GR|=3$), over the planning horizon ($|T|=10$). The size of the MILP problem is summarised in Table 2, where case iii is the base scenario (Section 6) and the other cases are variations with different transportation and CCS assumptions (Sections 7 and 8).

With the computational potential of current machines and the advances in MINP solvers, the full-space problem can be solved in reasonable computational times (*e.g.* the base scenario is solved with an optimality gap of 7.5% in less than 13 h). However, it is possible to reduce the CPU times and obtain better values of the objective function through hierarchical procedures. These kinds of methods have been presented previously in the literature (Agnolucci et al., 2013; Sabio et al., 2010), based on the fact that the relaxation of integer variables, especially if they take large values, tends to be tight and leads to solutions very close to the full-space optimal solution. Specifically, a two-step hierarchical procedure is used in SHIPMod extension.

The first step consists of the solution of a relaxed problem to determine the location, scale and technology of production plants over time. With this purpose, let x_1 be the set of continuous variables x of the problem described by Eq. (20), including the relaxed number of storage facilities (NS_{isjgt}), filling stations (NF_{ifjgt}), and road transportation units (\overline{NTU}_{ilgt} , $\overline{NTU}_{ilgg't}$), in addition to the continuous variables of the model. Thus, let X_1 be the set of integer decisions X , which only contains the number of production facilities (NP_{ipjgt}) in this stage. In the second step, a reduced version of the problem is solved by fixing from step 1 the number of plants over the planning horizon to determine the exact number of storage facilities, filling stations and road transportation units and update all the other optimisation variables. Let x_2 be now the set of continuous variables x of the problem of Eq. (20), composed of the genuine

continuous variables of the model, and let X_2 be the set of integer variables X , now comprising NS_{isjgt} , NF_{ifjgt} , \overline{NTU}_{ilgt} and $\overline{NTU}_{ilgg't}$ and excluding the number of plants, which are fixed.

The optimisation problems presented in the following Sections have been solved in GAMS 24.4 (GAMS, 2014) using CPLEX 12.6 solver on a 3.5 GHz, 32 GB of RAM machine (Intel® Xeon® Processor E51650). The optimality gaps have been set to 5% and 1% for the first and second step, respectively. Additionally, the maximum memory space for the branch and cut tree has been restricted to 30,000 MB and the maximum CPU time has been limited to 20 h in 8 parallel threads in each optimisation step.

5. Hydrogen fuelling infrastructure in the UK

The rest of the paper analyses the optimal infrastructure for satisfying the hydrogen demand in the passenger transport sector in the UK over the next decades using the extended SHIPMod. The forecasted increase of hydrogen consumption is defined exogenously according to the logistic demand diffusion model by Agnolucci and McDowall (2013), assuming that there are 2.5% of innovators by 2035 and hydrogen vehicles ultimately get to the totality of the market, as represented in Fig. 4(b). Specifically, the transition from 2020 to 2070 is studied, reaching a 50% of hydrogen penetration and a consumption of 5000 tonnes H₂ d⁻¹. It is solved using 5-year time periods. Moreover, the overall demand is distributed in 36 regions according to the UK demographic data. The spatial discretisation is illustrated in Fig. 4(a) and corresponds to the Nomenclature of Territorial Units for Statistics (NUTS) level 2 (Eurostat, 2013), where the five original zones for Inner and Outer London (UKI3, UKI4, UKI5, UKI6, and UKI7) are combined into one single region. The adoption behaviour in each area depends on socio-economic attributes, which determine whether hydrogen is introduced in 2020 or 2030 with an earlier or later diffusion, respectively (Agnolucci and McDowall, 2013). Existing hydrogen facilities and transportation modes are not considered to be available for this case study. International LH₂ can be imported in the six major UK liquid freight ports, identified from DfT (2014). Finally, the problem considers three offshore reservoirs located in the Irish Sea and the North Sea for CO₂ sequestration. The data have been collected from multiple sources, such as (DECC, 2014a, 2015; Dodds and McDowall, 2012; DOE, 2010). Details can be found in the Supplementary Material.

6. Role of transition time horizons

The optimum deployment of the hydrogen production and delivery infrastructure is solved using a present value cash flow analysis with different discount rates to evaluate their effect in the progression of the HSC investments. A first case is defined by a discount rate of 3.5%, which corresponds to the recommended value by the HM Treasury for measuring the economic efficiency of long-term investment projects of public agencies (HM Treasury, 2011). The problem is also studied with a discount rate of 10% to provide a shareholder point of view. The MILP problem is composed in both cases of 74,574 equations and 86,731 variables, from which 28,740 are discrete. It is solved in 0.2 and 9.1 h, respectively.

As illustrated in Figs. 5(a) and 6(a), which present the evolution of the optimal infrastructure for both discount rates, LH₂ is only used for imports in Northern Ireland (NO) and East Yorkshire/Northern Lincolnshire (E1) whereas all domestically-produced hydrogen in mainland regions is GH₂. Specifically, SMR is the cheapest production technology. In the first stages of the transition, a medium-size manufacturing facility is installed in a central location – Bedfordshire and Hertfordshire (H2) with 3.5% discount rate and Berkshire, Buckinghamshire and Oxfordshire (J1) with 10%

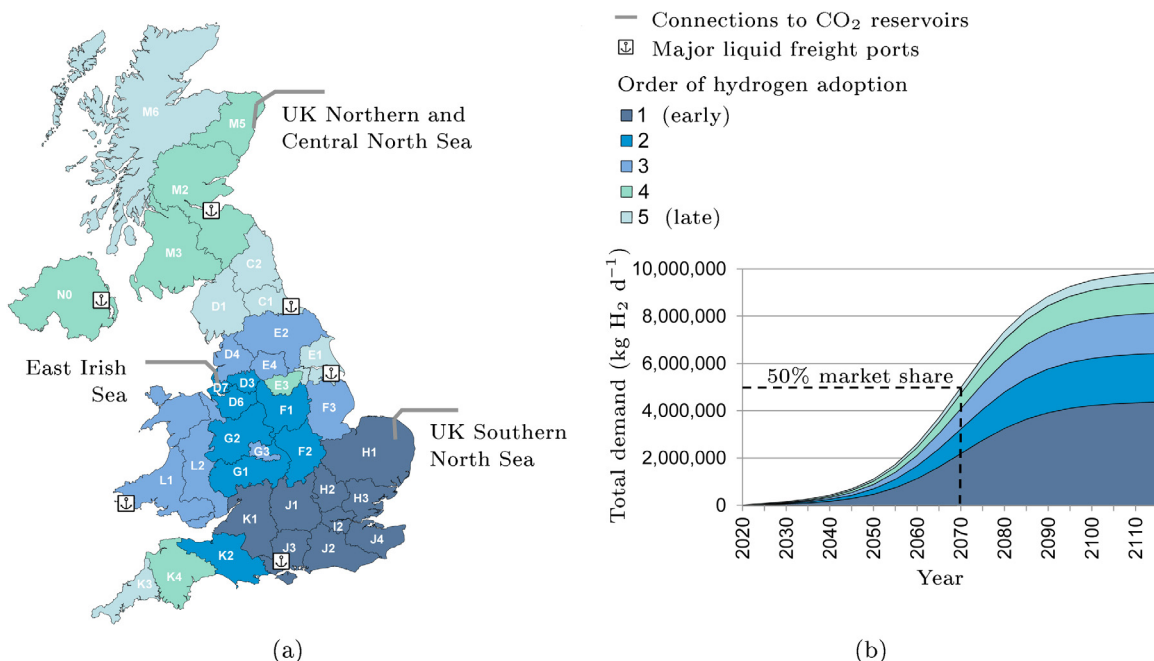


Fig. 4. Spatial discretisation of the demand: (a) regions by order of hydrogen adoption, international import locations and CO₂ collection points and (b) logistic diffusion model (Agnolucci and McDowall, 2013).

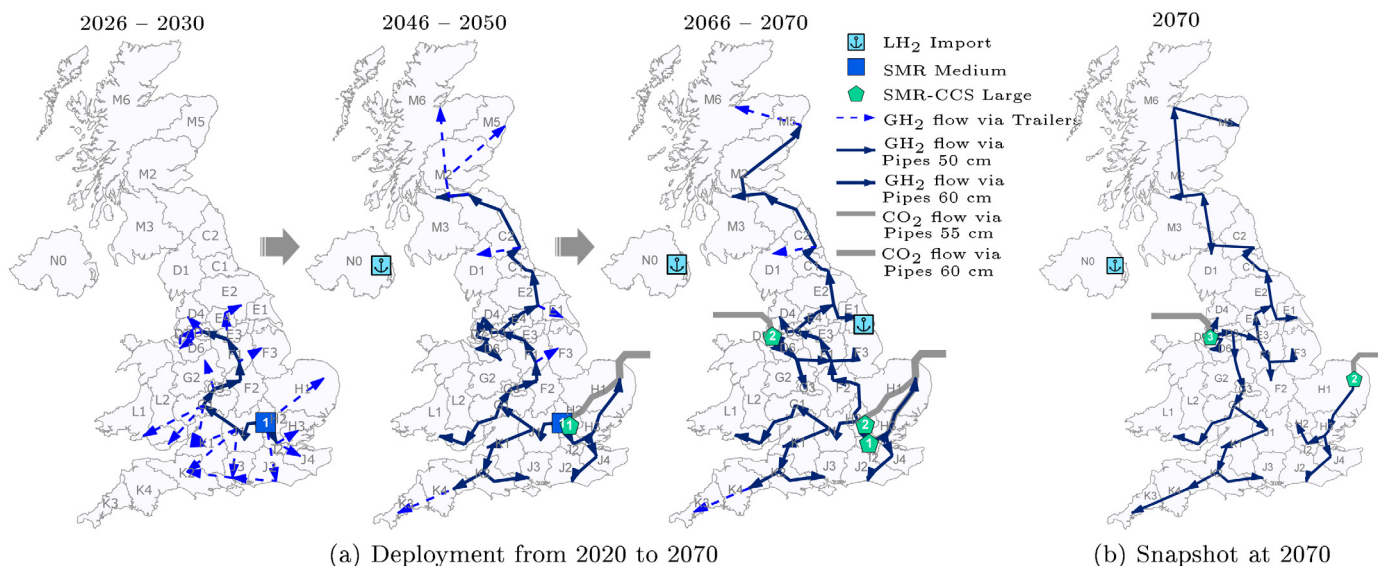


Fig. 5. Evolution of the HSC infrastructure over time in the base case with a discount rate of 3.5%.

– to facilitate the hydrogen supply to early adoption regions. Subsequently, several large-scale plants with carbon capture are installed relatively close to the CO₂ collection points of the East Irish Sea and Southern North Sea reservoirs to face the increasing hydrogen demand and tightening emission targets. So, all production plants are gathered around North-West and South-East England. Hydrogen is initially carried by trailers and progressively transported via pipelines.

The profiles of hydrogen import and production by technology and scale, presented in Fig. 7, are equivalent in both cases, as well as the production installed capacity, detailed in Fig. S5 of the Supplementary Material. In contrast, higher discount rates represent a choice for delaying transportation capital expenditure, notably investments in hydrogen and CO₂ pipes, as illustrated in Fig. 8. Lower discount rates tend to anticipate the rising hydrogen demand

in the following decades and lead to a faster construction of fully developed pipeline networks. For instance, hydrogen transmission pipes in the period 2036–2040 already consist of 1460 km with 3.5% discount rate whereas only 580 km have been established with a value of 10%. The length of installed hydrogen pipelines over time is detailed in Fig. S6 of the Supplementary Material.

The total cost of building the hydrogen infrastructure network is £ 15,281 million and £ 3180 million for the scenarios with discount rates of 3.5% and 10%, respectively. The cost contributions are summarised in Table 1 and Fig. 9. With a higher discount rate, the percentage of road transportation expenses increases significantly. Additionally, the operating cost of facilities is reduced from 66% to 50% due to the smaller effect of later years – with higher production rates – while the capital cost increases from 14% to 22% due to the larger influence of early years – with more investments. This

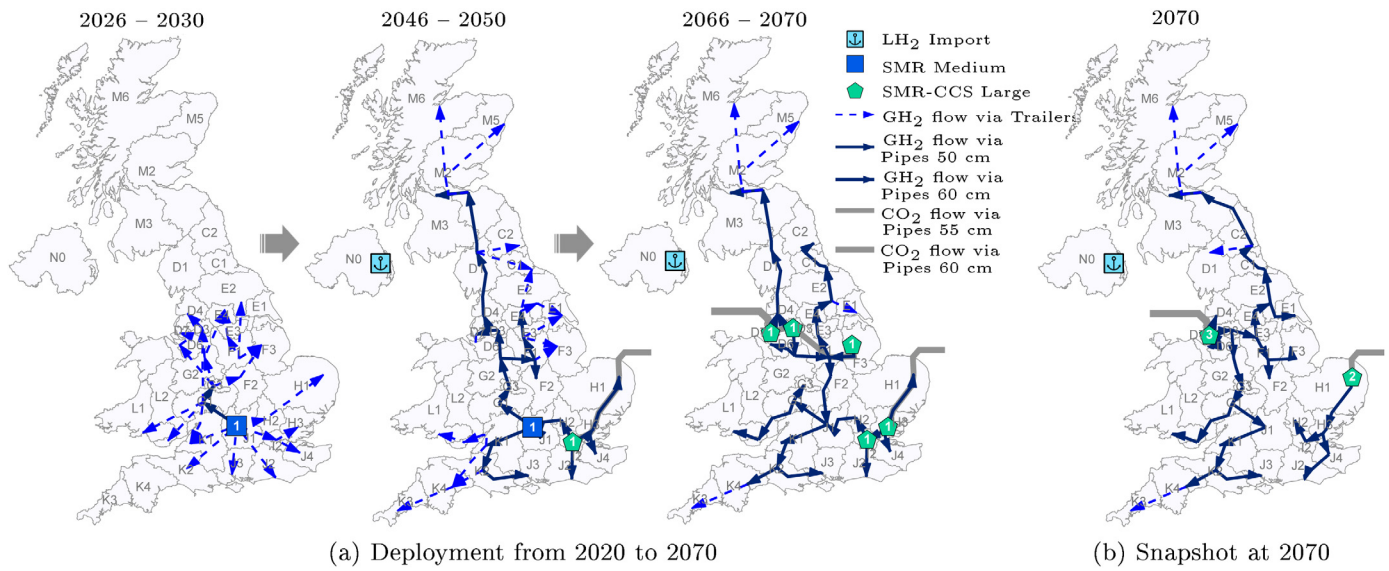


Fig. 6. Evolution of the HSC infrastructure over time in the base case with a discount rate of 10%.

Table 1

Present value of the cost contributions of the optimal hydrogen infrastructure with discount rates of 3.5% and 10% (base case), in m£.

	Discount rate 3.5%	Discount rate 10%
Total cost	15,281	3180
Capital cost of facilities	2213	703
Capital cost of pipelines	1340	285
Capital cost of road transport	75	72
Operating cost of facilities	10,122	1579
Operating cost of pipelines	75	14
Operating cost of road transport	477	377
Cost of carbon emissions	191	44
Cost of international imports	790	105

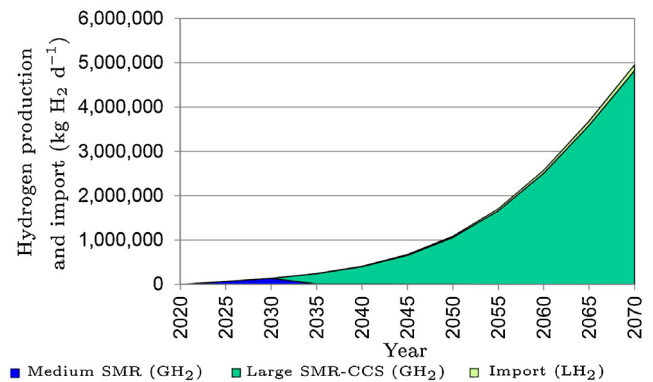


Fig. 7. Evolution of the hydrogen domestic production and international import over time in the base case with discount rates of 3.5% and 10%.

behaviour is illustrated in Figs. S7 and S8 of the Supplementary Material, together with the delay in pipeline capital charges. The cost of hydrogen production and delivery per unit is in the range of 5.3–2.1 £/kg H₂ and 3.7–2.0 £/kg H₂ before 2050, respectively. These values are below the 3.52 £/kg H₂ European reference for 2050 according to a study by McKinsey (2010), thus confirming the economic viability of the HSC infrastructure.

In terms of environmental impact, the optimal configurations based on SMR allow the consumption of cheap fossil fuels and yet reduce CO₂ emissions through the establishment of CCS. This is a challenging intermediate solution to mitigate global warming before the required increase of renewable energies and reduction

of their technological cost is achieved. The obtained CO₂ outflow is represented in Fig. 13, compared to the GHG emission target for hydrogen fuelled passenger vehicles in the UK. This target is calculated from the total emission budgets established by the UK Government (CCC, 2014, 2015; DECC, 2014b; HM Parliament, 2008) and the hydrogen diffusion over the planning horizon, as detailed in Moreno-Benito et al. (2016). The graphic shows that the obtained outflows are compliant with the 2050 EU environmental targets. In

Table 2

Problem size and computational performance of cases i–vii and a–c solved with the two-stage hierarchical approach.

Case	No. equations	No. variables	No. discrete	No. Discrete		CPU time (h)		Optimality gap	
				Step 1	Step 2	Step 1	Step 2	Step 1	Step 2
i	74,574	86,731	23,460	13,180	13,380	20.0	0.1	8.2% ^a	0.7%
ii	70,574	80,891	26,340	16,060	16,260	5.2	1.2	5.0%	1.1% ^b
iii						7.0	2.1	4.9%	2.0% ^b
iv						20.0	2.2	5.2% ^a	2.5% ^b
v	74,574	86,731	28,740	18,460	18,660	20.0	2.6	5.5% ^a	2.3% ^b
vi						5.0	2.0	4.5%	1.4% ^b
vii						0.4	3.4	4.8%	1.0% ^b
a						0.01	0.5	4.9%	0.8%
b	54,114	73,678	25,140	14,860	18,660	0.2	1.4	4.9%	1.0%
c						0.1	0.9	4.5%	1.0%

^a Terminated by CPU time limit (20 h).

^b Terminated by tree memory limit (30,000 MB).

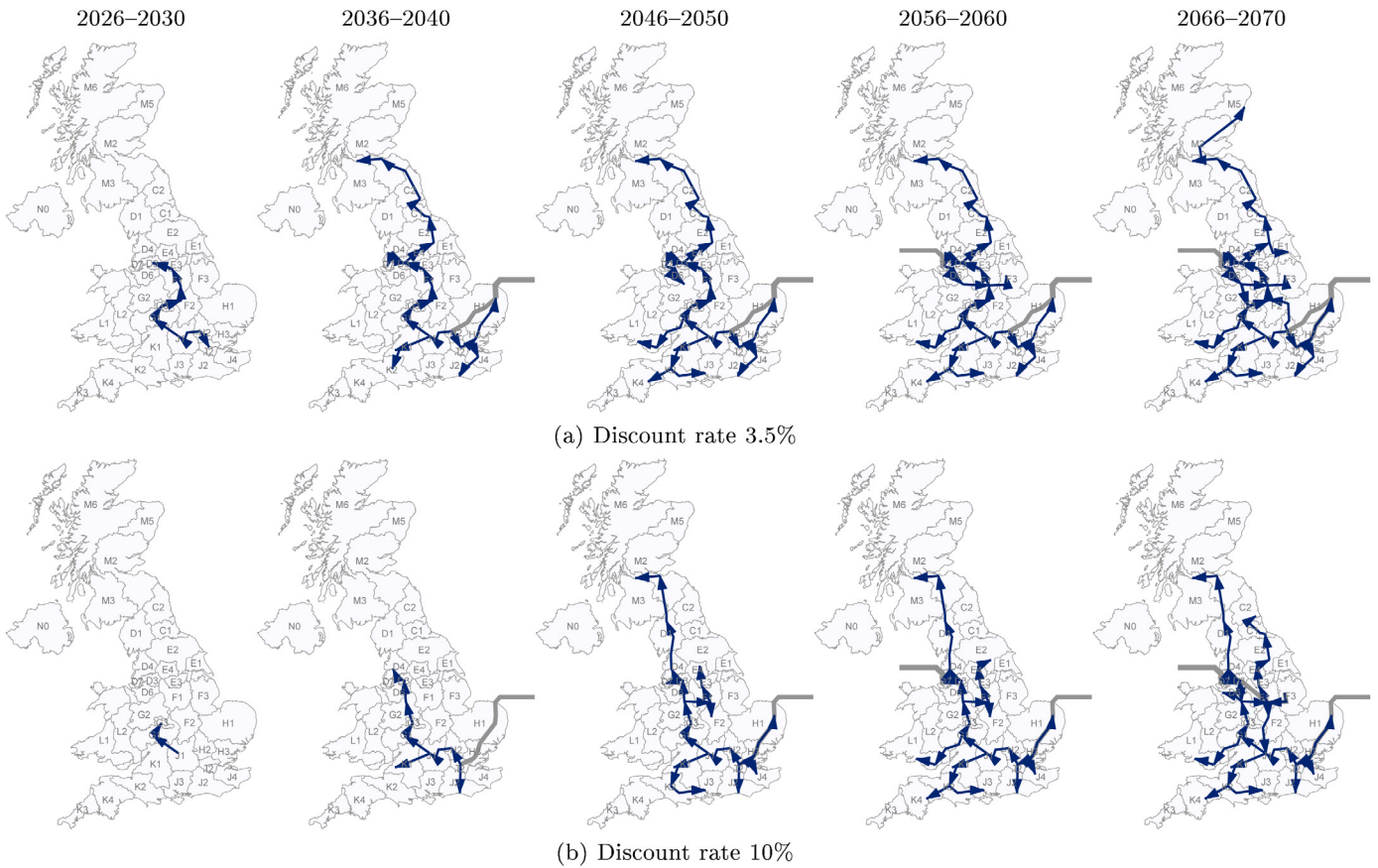


Fig. 8. Deployment of hydrogen and CO₂ pipeline networks over time in the base case with discount rates of 3.5% and 10%.

fact, the optimal configuration reduces the CO₂ emissions of hydrogen fuelled vehicles after 2030 in more than the 95% compared to the 1990 values. Regarding the reservoir usage, the CO₂ sequestration does not deplete more than the 1.3% of their maximum capacity during the studied planning horizon of 50 years.

Finally, the evolution of the infrastructure in the planning horizon from 2020 to 2070 is compared with the snapshot solution at 2070 covering the final demand. Such a problem is addressed by minimising the total cost annuities, and the corresponding MILP problem has 7488 equations and 11,293 variables, from which 2874 are discrete. Since the extended SHIPMod assumes a perfect foresight, the snapshot solution is similar to the deployed infrastructure

at the end of the planning horizon, as shown in Figs. 5(b) and 6(b). However, this solution does not incorporate strategic decisions like the selection of central locations for the early SMR plants to reduce hydrogen delivery costs via trailers. The initial plants are later replaced by larger facilities with CCS but still determine the infrastructure echelons in the deployment problem.

7. Role of transportation modes

The hydrogen delivery alternatives for the different stages of the transition are here analysed assuming a discount rate of 10%. The following transport situations are considered: (i) only

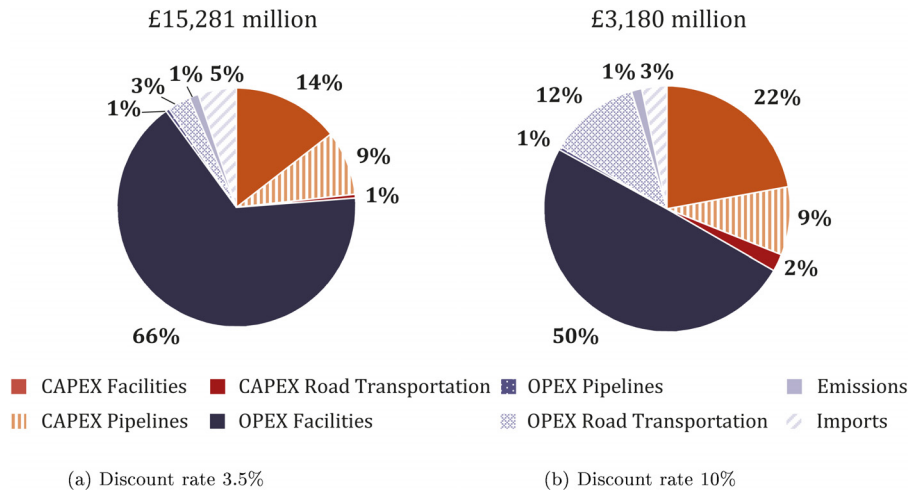


Fig. 9. Percentage of the discounted cost contributions of the optimal HSC infrastructures in the base case with discount rates of 3.5% and 10%, in % of the total cost.

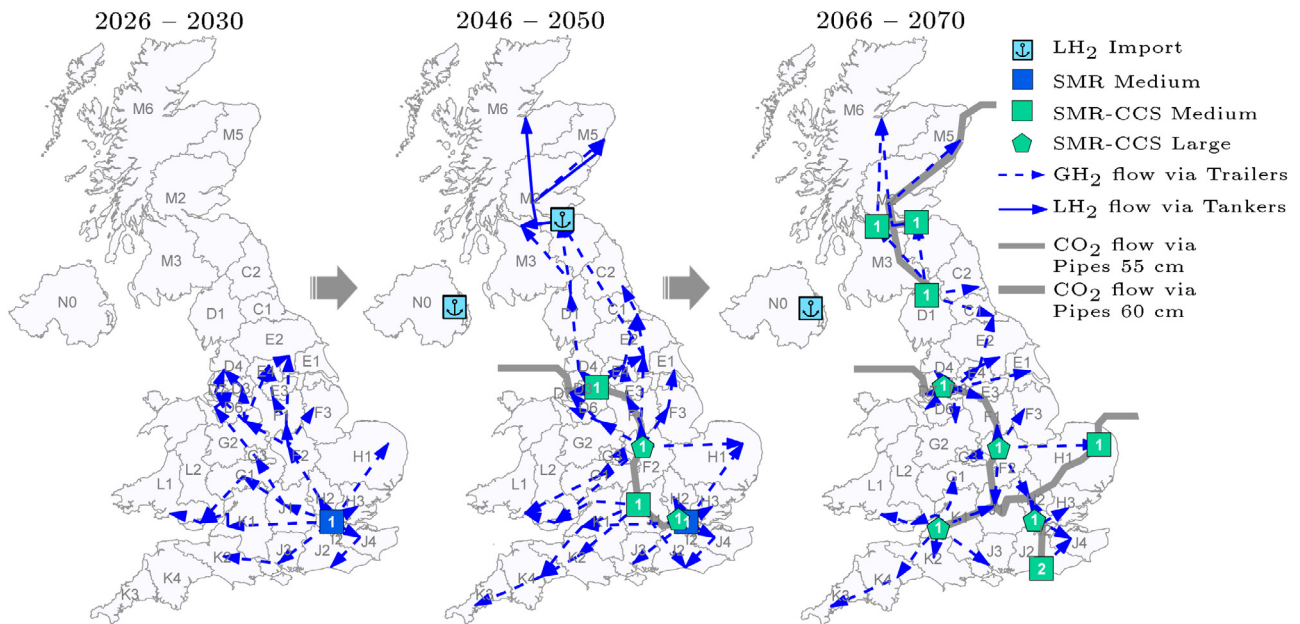


Fig. 10. Evolution of the HSC infrastructure over time in the scenario without pipelines with a discount rate of 10% (case i).

road transportation is permitted, (ii) a limited number of pipeline connections are allowed, which correspond to the existing natural gas infrastructure, (iii) all neighbouring pipeline connections are permitted – *i.e.* base case presented above, (iv) and (v) base case with 27% and 50% higher pipeline capital costs, and (vi) and (vii) base case with 27% and 50% lower pipeline capital costs. The corresponding MILP size and computational performance are presented in Table 2. In all cases, the two-step hierarchical approach can find feasible solutions, but cannot always converge within the CPU time limit and the branch and cut memory limit below the optimality gaps of 5% and 1% set for the first and the second steps. The more computationally expensive scenarios are those with tighter trade-offs between compressed versus liquid hydrogen and between centralised versus distributed production, such as cases i, iv and v. These are the scenarios without pipelines or with higher pipeline capital costs where other, less-efficient, delivery options become more relevant.

The optimal infrastructure deployment without pipelines (case i) is shown in Fig. 10. This solution, with a total cost of £ 3510 million, is around a 10% costlier than the optimal solution of the base scenario (case iii). When pipelines are not allowed, the next more efficient solution is obtained by reducing the scale of compressed hydrogen production via SMR to locate several medium-sized plants in scattered sites and hence reduce the road delivery costs. The 24% of SMR production with CCS is now produced at medium scale instead of large size. Additionally, the port region in Eastern Scotland (M2) is backed by liquid hydrogen imports in some periods. Overall, Fig. 10 shows a predominance of GH_2 generation and its delivery via trailers. In contrast, a preliminary study without pipelines and lower electricity costs – resulting in smaller liquefaction expenses – provided an optimal solution based on LH_2 production to increase the hydrogen volumetric energy and use LH_2 tankers for its transportation. In this case, large-scale centralised plants close to CO_2 collection points were obtained, likewise the scenario with pipelines. Summarising, the selection of GH_2 versus LH_2 mostly depends on the available transportation modes and the electricity price for liquefaction.

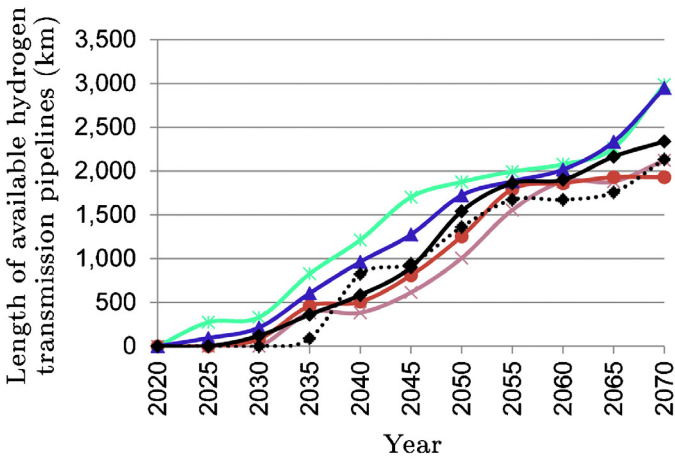
In all the remaining scenarios with pipelines, the optimal solutions include this option as the principal delivery mode. However, the timing and extent of the construction of the pipeline network

depend on the capital investment required. Fig. 11 shows the evolution of the constructed length of hydrogen pipelines in scenarios ii to vii. Essentially, larger pipeline capital costs lead to a later pipeline construction, like cases iv and v, while more mature networks are obtained in those scenarios with lower pipeline capital costs, like iii, vi and vii. In all cases, the pipeline infrastructure is nearly complete by 2055. Regarding local pipelines, their construction is slower than regional ones, as the required capital investment becomes ineffective for small flow rates and short distances.

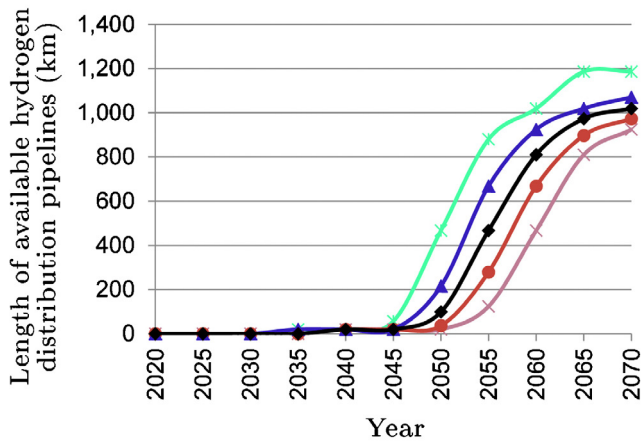
The cost contributions of the optimal HSC infrastructures of these scenarios are summarised in Table 3. There is a rise in road transportation expenses with an increase in pipeline capital costs per length, which is due to the higher use of trailers. Pipeline expenditure is adjusted by delaying pipeline investments in scenarios with higher capital cost. Besides, those cases with more expensive transportation modes, namely i, ii and v, lead to higher carbon emission expenses because they include the construction of more than one medium-sized SMR production plant without CCS to save transportation charges in early periods. However, the solution with the higher road transportation costs is the one without pipelines, despite the higher spatial distribution of hydrogen manufacturing facilities. The pipeline expenses in this scenario are the ones associated with CO_2 pipelines.

8. Role of carbon capture and storage

The optimal hydrogen supply chains of all the scenarios studied in previous sections rely almost entirely on the use of natural gas reforming with carbon sequestration. The importance of including CCS systems is analysed next by comparing the base case with three scenarios without carbon sequestration and different hydrogen import allowance levels: (a) unlimited international import, and (b) and (c) import limited by the 50% and 10% of the total hydrogen demand. The MILP size and computational performance of these scenarios are provided in Table 2. From this table, all scenarios a to c are solved within the predefined optimality gaps in CPU times of less than 2 h combining the two optimisation stages, showing a dependence of the computational performance on the elements included in the optimisation framework.



(a) Transmission pipelines

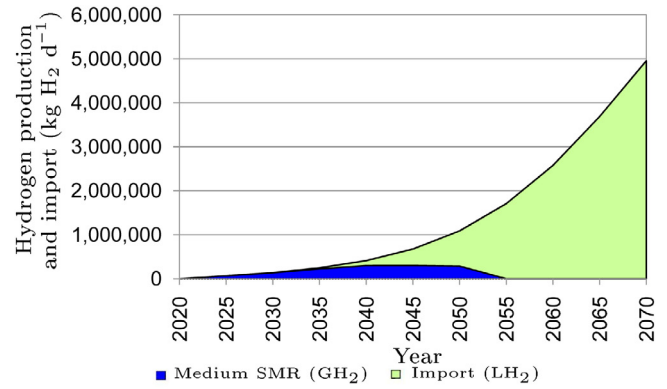


(b) Distribution pipelines

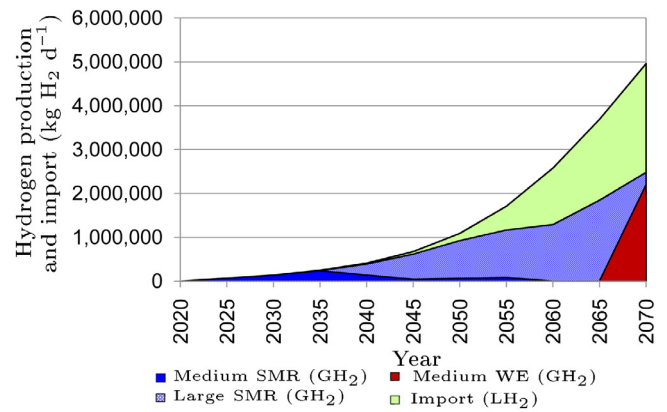
- ...◆ (ii) restricted connections
- ◆ (iii) base case
- (iv) 27% higher pipe cost
- × (v) 50% higher pipe cost
- ▲ (vi) 27% lower pipe cost
- * (vii) 50% lower pipe cost

Fig. 11. Evolution of the cumulative constructed length of hydrogen pipelines in the scenarios with different capital costs and potential connections with a discount rate of 10% (cases ii to vii).

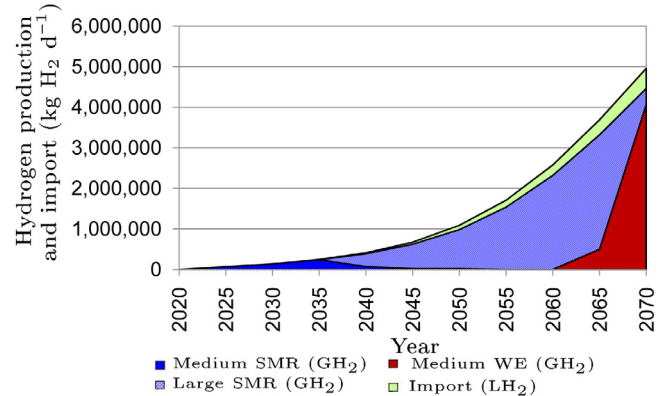
Without carbon capture, SMR is no longer the major alternative. The optimal solutions of the cases a, b and c rely on international imports and a combination of electrolysis and SMR domestic production, as represented in Fig. 12. The cheapest option without the possibility to capture and store the CO₂ emissions is the international import of liquid hydrogen. The next best option is electrolysis. Basically, there are three stages in the hydrogen infrastructure deployment, namely initial hydrogen production at medium scale from natural gas, which is followed by an increase in the production size, and a final substitution of SMR production by



(a) Unlimited international imports



(b) 50% maximum international import



(c) 10% maximum international import

Fig. 12. Evolution of the hydrogen domestic production and international import over time in the scenarios without CCS and different degrees of international imports allowance with a discount rate of 10% (cases a to c).

either international hydrogen imports or national production via electrolysis.

The total carbon emissions obtained in the base case and the three scenarios without CCS are represented in Fig. 13, compared to the GHG emission target for hydrogen fuelled passenger vehicles in the UK. The GHG emission targets are met in most cases, except for those without CCS and constrained imports. This is due to very tight GHG emission targets, which aim a reduction of the 80% from 2050 and beyond, as well as to the high expenses of technologies with lower emissions, as it could be electrolysis. Consequently, it is not until 2060 that WE is introduced in the production portfolio, what results in high CO₂ emissions generated by SMR without CCS. After 2060, an increase in the carbon price in the last periods of the

Table 3

Present value of the cost contributions of the optimal hydrogen infrastructure in cases i to vii with a discount rate of 10%, in m£.

	i	ii	iii	iv	v	vi	vii
Total cost	3503	3216	3180	3242	3274	3089	3007
Capital cost of facilities	736	687	703	702	702	702	702
Capital cost of pipelines	78	218	285	318	292	280	287
Capital cost of road transport	119	76	72	75	80	61	48
Operating cost of facilities	1607	1570	1579	1579	1579	1579	1579
Operating cost of pipelines	4	11	14	16	15	14	15
Operating cost of road transport	725	418	377	402	457	304	227
Cost of carbon emissions	112	132	44	44	44	44	44
Cost of international imports	122	105	105	105	105	105	105

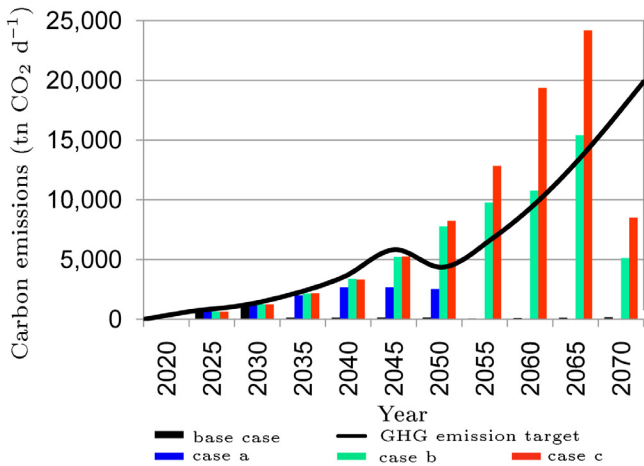


Fig. 13. GHG emission target and CO₂ emissions in the base case and cases a to c without CCS and (a) unlimited international import, (b) 50% maximum international import and (c) 10% maximum international import, all of them with a discount rate of 10%.

time horizon forces the replacement of SMR production by WE and a reduction in CO₂ emissions is accomplished. The late introduction of electrolysis in the case of CCS exclusion is likely to be supported by a larger capacity of renewables.

Table 4

Present value of the cost contributions of the optimal hydrogen infrastructure in cases a, b and c with a discount rate of 10%, in m£.

	a	b	c
Total cost	4842	4956	5094
Capital cost of facilities	562	653	734
Capital cost of pipelines	24	149	193
Capital cost of road transport	66	71	61
Operating cost of facilities	668	1329	1680
Operating cost of pipelines	1	8	10
Operating cost of road transport	326	363	332
Cost of carbon emissions	381	1359	1752
Cost of international imports	2814	1023	332

Regarding the spatial distribution of the HSC, Fig. 14 illustrates the decentralisation of hydrogen production via medium-scale SMR and electrolysis in the deployment of the optimal hydrogen infrastructure of scenario c. Hydrogen delivery is based on a combination of compressed hydrogen initially transported via trailers and later via pipelines, and liquid hydrogen carried by tankers. Finally, Table 4 summarises the cost contributions of the optimal HSC infrastructure for each of these cases, and shows an increase in capital and operating costs of facilities, pipelines and carbon emissions when more restrictive constraints on hydrogen import are established. The total infrastructure expenses are between the 52% and 60% higher than the base case iii.

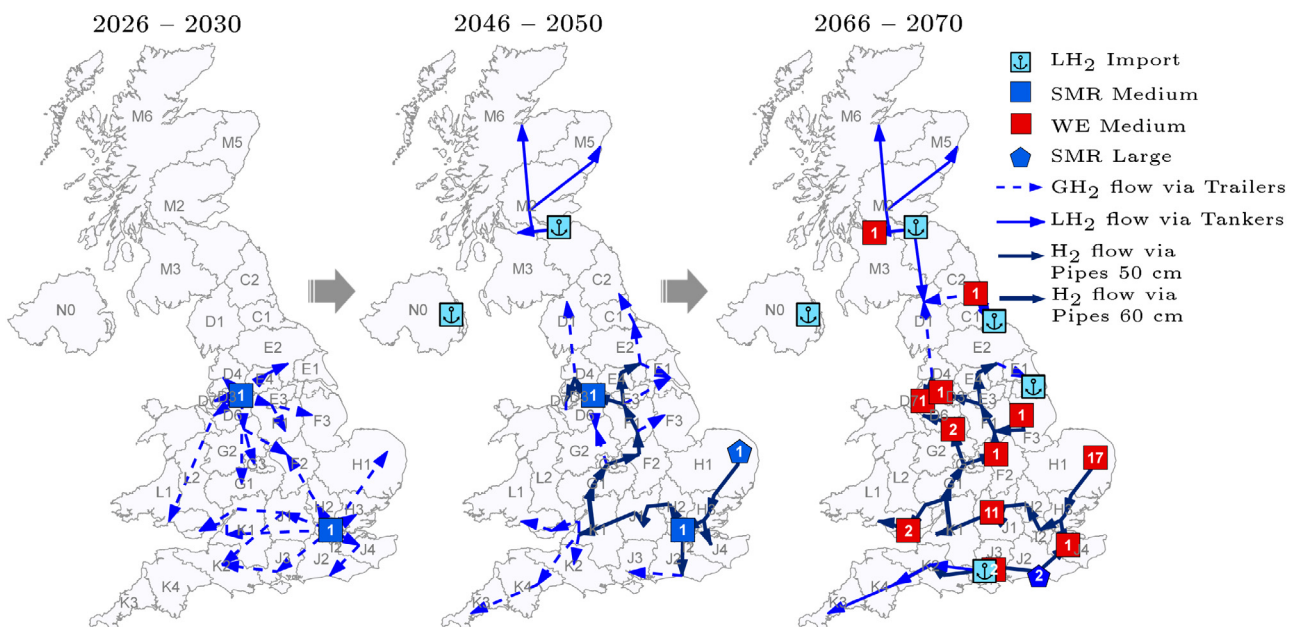


Fig. 14. Evolution of the HSC infrastructure over time in the scenario without CCS and 10% maximum international import with a discount rate the 10% (case c).

9. Conclusions

This work extends the optimisation-based framework SHIPMod for the design of the hydrogen supply chain infrastructure. In addition to the consideration of economies of scale and CCS technologies for solving the transition towards low-carbon energy systems, this contribution includes the mathematical formulation for solving the transportation via pipelines at local and regional scales and international imports, as well as the deactivation of the elements of the infrastructure after their useful life has been completed, given the timeframes of 50 years under study. This way, the trade-offs between centralised and distributed production, hydrogen pipelines and road transportation, production scales, production technologies, and product forms, have been included in the multi-period spatial-explicit MILP formulation. Most importantly, the extended optimisation framework provides a quantitative analysis tool to evaluate the infrastructure components at different phases of the transition towards a sustainable low-carbon hydrogen economy. This is crucial to understand the alternative options for introducing hydrogen in the energy system over the next decades.

The optimal hydrogen production and delivery network that satisfies the hydrogen demand in the transport sector in the next 50 years has been solved with different modelling assumptions. Essentially, hydrogen production from natural gas through SMR with CCS is posed to be the most cost-effective alternative that maintains a low level of carbon emissions. The time preference represented in the discount rate mostly affects to the development pace and the extent of the pipeline network construction, but not to the production type, the hydrogen form, or the percentage of international imports. Similarly, the capital costs of the pipelines uniquely affects the progress of the pipeline network, while the unavailability of pipelines leads to the diversification of hydrogen production in a larger number of SMR plants with a smaller scale, in order to reduce the regional transportation via compressed hydrogen trailers in the whole timeframe. It is interesting that the same profiles of international hydrogen import and national production by technology type are equivalent in all cases, independently of the delivery mode. In contrast, the elimination of the CCS system involves more changes in the production figures. As the system cannot rely on SMR without carbon sequestration due to the high costs of CO₂ emissions, the solution includes the import of hydrogen as a first option, followed by the use distributed electrolysis, powered by intermittent renewable energy sources among others, as a second alternative. By studying the role of the delivery mode and the CCS system, the influence of plant scales becomes notable, as smaller scales are used to balance the increment of transportation costs.

To conclude, the extended SHIPMod constitutes an extensive optimisation framework for solving hydrogen infrastructure deployments with a hierarchical strategy that leads to feasible solutions close to the true optimal solution in reasonable computational times. This work has focused on the economic optimisation of the HSC infrastructure for the passenger sector in the UK, but the proposed framework can also be applied to the analysis of other future hydrogen economies. As future steps, other procedures for addressing the infrastructure flexibility in front of uncertain hydrogen demand forecasts could be studied. The introduction of intra-day and inter-seasonal hydrogen storage dynamics for modelling the hydrogen consumption and supply mismatches in the optimisation framework is also a challenging step to be taken. Finally, alternative optimisation methods that lead to more efficient solution procedures could also be considered.

Acknowledgements

Financial support received from the Engineering and Physical Sciences Research Council (EPSRC) in the UK funding the project

‘Hydrogen’s value in the energy system (HYVE) – EP/L018284/1’ is acknowledged. The authors would also like to thank Dr. Paul E. Dodds and Mr. Andres J. Calderon for the useful discussions held during the development of this work.

Appendix A. Supplementary data

Supplementary data associated with this article can be found, in the online version, at <http://dx.doi.org/10.1016/j.compchemeng.2016.08.005>.

References

- Agnolucci, P., Akgul, O., McDowall, W., Papageorgiou, L.G., 2013. The importance of economies of scale, transport costs and demand patterns in optimising hydrogen fuelling infrastructure: an exploration with SHIPMod (spatial hydrogen infrastructure planning model). *Int. J. Hydrogen Energy* 38, 11189–11201.
- Agnolucci, P., McDowall, W., 2013. Designing future hydrogen infrastructure: insights from analysis at different spatial scales. *Int. J. Hydrogen Energy* 38, 5181–5191.
- Akgul, O., Shah, N., Papageorgiou, L.G., 2012. An optimisation framework for a hybrid first/second generation bioethanol supply chain. *Comput. Chem. Eng.* 42, 101–114.
- Akgul, O., Zamboni, A., Bezzo, F., Shah, N., Papageorgiou, L.G., 2011. Optimization-based approaches for bioethanol supply chains. *Ind. Eng. Chem. Res.* 50, 4927–4938.
- Almansoori, A., Shah, N., 2009. Design and operation of a future hydrogen supply chain: multi-period model. *Int. J. Hydrogen Energy* 34, 7883–7897.
- Almansoori, A., Shah, N., 2012. Design and operation of a stochastic hydrogen supply chain network under demand uncertainty. *Int. J. Hydrogen Energy* 37, 3965–3977.
- André, J., Aurray, S., De Wolf, D., Memmah, M.-M., Simonnet, A., 2014. Time development of new hydrogen transmission pipeline networks for France. *Int. J. Hydrogen Energy* 39, 10323–10337.
- Committee on Climate Change (CCC), 2014. Meeting Carbon Budgets – 2014 Progress Report to Parliament. *Tech. rep. CCC, London*.
- Committee on Climate Change (CCC), 2015. The Fifth Carbon Budget. The next step towards a low-carbon economy. *Tech. rep. CCC, London*.
- Čuček, L., Martín, M., Grossmann, I.E., Kravanja, Z., 2014. Multi-period synthesis of optimally integrated biomass and bioenergy supply network. *Comput. Chem. Eng.* 66, 57–70.
- d’Amore, F., Bezzo, F., 2016. Strategic optimisation of biomass-based energy supply chains for sustainable mobility. *Comput. Chem. Eng.* 87, 68–81.
- Dayhim, M., Jafari, M.A., Mazurek, M., 2014. Planning sustainable hydrogen supply chain infrastructure with uncertain demand. *Int. J. Hydrogen Energy* 39, 6789–6801.
- De-León Almaraz, S., Azzaro-Pantel, C., Montastruc, L., Boix, M., 2015. Deployment of a hydrogen supply chain by multi-objective/multi-period optimisation at regional and national scales. *Chem. Eng. Res. Des.* 104, 11–31.
- De-León Almaraz, S., Azzaro-Pantel, C., Montastruc, L., Domenech, S., 2014. Hydrogen supply chain optimization for deployment scenarios in the Midi-Pyrénées region, France. *Int. J. Hydrogen Energy* 39, 11831–11845.
- Department of Energy and Climate Change (DECC), 2014a. Updated Energy & Emissions Projections. Annex M: Growth assumptions and prices. *Tech. rep. DECC, London*.
- Department of Energy and Climate Change (DECC), 2014b. Updated energy and emissions projections 2014. *Tech. rep. DECC, London*.
- Department of Energy and Climate Change (DECC), 2015. Quarterly Energy Prices, Table 3.1.4. *Tech. rep. DECC, London*.
- Department for Transport (DfT), 2014. Port freight statistics: 2014 final figures report. *Tech. rep. DfT, London*.
- Dodds, P.E., McDowall, W., 2012. A review of hydrogen delivery technologies for energy system models. UKSHEC Working Paper No. 7. *Tech. rep. UCL Energy Institute, University College London*.
- Department of Energy (DOE), 2010. The Hydrogen Analysis (H2A) Project Delivery Components Model Version 2.0. *Tech. rep. National Renewable Energy Laboratory, DOE, Golden, Colorado*.
- Ekins, P., Hughes, N., 2009. The prospects for a hydrogen economy (1): hydrogen futures. *Technol. Anal. Strateg. Manag.* 21, 783–803.
- Elahi, N., Shah, N., Korre, A., Durucan, S., 2014. Multi-period least cost optimisation model of an integrated carbon dioxide capture transportation and storage infrastructure in the UK. *Energy Proc.* 63, 2655–2662.
- Eurostat, 2013. Nomenclature of Territorial Units for Statistics (NUTS). ec.europa.eu/eurostat/web/nuts/overview [accessed on 26/02/2016].
- Floudas, C.A., Niziolek, A.M., Onel, O., Matthews, L.R., 2016. Multi-scale systems engineering for energy and the environment: challenges and opportunities. *AIChE J.* 62, 602–623.
- GAMS, 2014. The Solver Manuals, GAMS Release 24.4.1. *Tech. rep. GAMS Development Corporation, Washington, DC, USA*.

- Giarola, S., Zamboni, A., Bezzo, F., 2011. Spatially explicit multi-objective optimisation for design and planning of hybrid first and second generation biorefineries. *Comput. Chem. Eng.* 35, 1782–1797.
- Guillén-Gosálbez, G., Mele, F.D., Grossmann, I.E., 2010. A bi-criterion optimization approach for the design and planning of hydrogen supply chains for vehicle use. *AIChE J.* 56, 650–667.
- Han, J.-H., Ryu, J.-H., Lee, I.-B., 2012. Modeling the operation of hydrogen supply networks considering facility location. *Int. J. Hydrogen Energy* 37, 5328–5346.
- Han, J.-H., Ryu, J.-H., Lee, I.-B., 2013. Multi-objective optimization design of hydrogen infrastructures simultaneously considering economic cost, safety and CO₂ emission. *Chem. Eng. Res. Des.* 91, 1427–1439.
- HM Parliament, 2008. The Climate Change Act 2008. Tech. rep. Department of Energy and Climate Change (DECC), London.
- HM Treasury, 2011. The Green Book. Appraisal and Evaluation in Central Government. Tech. rep. Treasury Guidance, London.
- Hugo, A., Rutter, P., Pistikopoulos, S., Amorelli, A., Zoia, G., 2005. Hydrogen infrastructure strategic planning using multi-objective optimization. *Int. J. Hydrogen Energy* 30, 1523–1534.
- Johnson, N., Ogden, J., 2012. A spatially-explicit optimization model for long-term hydrogen pipeline planning. *Int. J. Hydrogen Energy* 37, 5421–5433.
- Kamarudin, S.K., Daud, W.R.W., Yaakub, Z., Misron, Z., Anuar, W., Yusuf, N.N.A.N., 2009. Synthesis and optimization of future hydrogen energy infrastructure planning in Peninsular Malaysia. *Int. J. Hydrogen Energy* 34, 2077–2088.
- Kim, J., Lee, Y., Moon, I., 2008. Optimization of a hydrogen supply chain under demand uncertainty. *Int. J. Hydrogen Energy* 33, 4715–4729.
- Konda, N.M., Shah, N., Brandon, N.P., 2011. Optimal transition towards a large-scale hydrogen infrastructure for the transport sector: the case for the Netherlands. *Int. J. Hydrogen Energy* 36, 4619–4635.
- Konda, N.M., Shah, N., Brandon, N.P., 2012. Dutch hydrogen economy: evolution of optimal supply infrastructure and evaluation of key influencing elements. *Asia-Pacific J. Chem. Eng.* 7, 534–546.
- Li, Z., Gao, D., Chang, L., Liu, P., Pistikopoulos, E.N., 2008. Hydrogen infrastructure design and optimization: a case study of China. *Int. J. Hydrogen Energy* 33, 5275–5286.
- Liu, P., Georgiadis, M.C., Pistikopoulos, E.N., 2011. Advances in energy systems engineering. *Ind. Eng. Chem. Res.* 50, 4915–4926.
- Marbán, G., Valdés-Solís, T., 2007. Towards the hydrogen economy? *Int. J. Hydrogen Energy* 32, 1625–1637.
- Marvin, W.A., Schmidt, L.D., Daoutidis, P., 2013. Biorefinery location and technology selection through supply chain optimization. *Ind. Eng. Chem. Res.* 52, 3192–3208.
- McKinsey, 2010. A portfolio of power-trains for Europe: a fact-based analysis. Tech. rep. Coordinated by McKinsey & Company, Available at: www.fch-ju.eu/sites/default/files/documents/Power.trains.for.Europe.pdf [accessed on 22/04/2016].
- Middleton, R.S., Bielicki, J.M., 2009. A scalable infrastructure model for carbon capture and storage: SimCCS. *Energy Policy* 37, 1052–1060.
- Moreno-Benito, M., Agnolucci, P., McDowall, W., Papageorgiou, L.G., 2016. Towards a sustainable hydrogen economy: role of carbon price for achieving GHG emission targets. In: Kravanja, Z. (Ed.), Proceedings of the 26th European Symposium on Computer Aided Process Engineering. *Computer Aided Chemical Engineering* 38, pp. 1015–1020.
- Sabio, N., Gadalla, M., Guillén-Gosálbez, G., Jiménez, L., 2010. Strategic planning with risk control of hydrogen supply chains for vehicle use under uncertainty in operating costs: a case study of Spain. *Int. J. Hydrogen Energy* 35, 6836–6852.
- Sabio, N., Kostin, A., Guillén-Gosálbez, G., Jiménez, L., 2012. Holistic minimization of the life cycle environmental impact of hydrogen infrastructures using multi-objective optimization and principal component analysis. *Int. J. Hydrogen Energy* 37, 5385–5405.
- Samsatli, S., Staffell, I., Samsatli, N.J., 2016. Optimal design and operation of integrated wind-hydrogen-electricity networks for decarbonising the domestic transport sector in Great Britain. *Int. J. Hydrogen Energy* 41, 447–475.
- Upchurch, C., Kuby, M., 2010. Comparing the *p*-median and flow-refueling models for locating alternative-fuel stations. *J. Transp. Geogr.* 18, 750–758.
- Voldsund, M., Jordal, K., Anantharaman, R., 2016. Hydrogen production with CO₂ capture. *Int. J. Hydrogen Energy* 41, 4969–4992.
- Yang, C., Ogden, J., 2007. Determining the lowest-cost hydrogen delivery mode. *Int. J. Hydrogen Energy* 32, 268–286.
- Yue, D., You, F., Snyder, S.W., 2014. Biomass-to-bioenergy and biofuel supply chain optimization: overview, key issues and challenges. *Comput. Chem. Eng.* 66, 36–56.